

DEC 28 '55

QC

983

A27

PR

# MONTHLY WEATHER REVIEW

VOLUME 83

NUMBER 9

SEPTEMBER 1955

## CONTENTS

	Page
An Investigation of Cyclone Development—Storm of December 13-15, 1951.....Lynn L. Means	185
Some Meteorological Aspects of Drought—With Special Reference to the Summers of 1952-54 over the United States.....Jerome Namias	199
The Weather and Circulation of September 1955.....Arthur F. Krueger	206
Some Small-Scale Features of the Track of Hurricane Ione Harold M. Jordan and David J. Stowell	210
Charts I-XV (Charts IV and V, Snowfall, omitted until November)	



U. S. DEPARTMENT OF COMMERCE • WEATHER BUREAU

# PUBLICATIONS OF THE U. S. WEATHER BUREAU

As the national meteorological service for the United States, the Weather Bureau issues several periodicals, serials, and miscellaneous publications on weather, climate, and meteorological science as required to carry out its public service functions. The principal periodicals and serials are described on this page and on the inside of the back cover. A more complete listing of Weather Bureau publications is available upon request to Chief, U. S. Weather Bureau, Washington 25, D. C.

Orders for publications should be addressed to the Superintendent of Documents, Government Printing Office, Washington 25, D. C.

## MONTHLY WEATHER REVIEW

First published in 1872, the *Monthly Weather Review* serves as a medium of publication for technical contributions in the field of meteorology, principally in the branches of synoptic and applied meteorology. In addition each issue contains an article descriptive of the atmospheric circulation during the month over the Northern Hemisphere with particular reference to the effect on weather in the United States. A second article deals with some noteworthy feature of the month's weather. Illustrated. Annual subscription: \$3.00; additional for foreign mailing, \$1.00; 30¢ per copy. Subscription to the *Review* does not include the *Supplements* which have been issued irregularly and are for sale separately.

## WEEKLY WEATHER AND CROP BULLETIN

Issued on Wednesday of each week, the bulletin covers the weather of the week and its effects on crops and farm activities. Short reports from individual States are supplemented by maps of average temperature and total precipitation. In the winter months a chart of snow depth is included. Annual subscription: \$3.00; additional for foreign mailing, \$1.00; 10¢ per copy. For period December through March: \$1.00; additional for foreign mailing, 50¢.

## CLIMATOLOGICAL DATA—NATIONAL SUMMARY

This monthly publication contains climatological data such as pressure, temperature, winds, rainfall, snowfall, severe storms, floods, etc., for the United States as a whole. A short article describing the weather of the month over the United States, tables of the observational data, and a description of flood conditions are supplemented by 15 charts. An annual issue summarizes weather conditions in the United States for the year. More detailed local data are provided in the *Climatological Data* (by sections) for 45 sections representing each State or a group of States and Hawaii, Alaska, and the West Indies. Annual subscription for either the National Summary or for a Section (including annual issue): \$4.00; additional for foreign mailing, \$1.50; 30¢ per monthly issue; 50¢ for annual issue alone.

(Continued on inside back cover)

The Weather Bureau desires that the *Monthly Weather Review* serve as a medium of publication for original contributions within its field, but the publication of a contribution is not to be construed as official approval of the views expressed.

The issue for each month is published as promptly as monthly data can be assembled for preparation of the review of the weather of the month. In order to maintain the schedule with the Public Printer, no proofs will be sent to authors outside of Washington, D. C.

The printing of this publication has been approved by the Director of the Bureau of the Budget, February 9, 1955.

# MONTHLY WEATHER REVIEW

JAMES E. CASKEY, JR., Editor

Volume 83  
Number 9

SEPTEMBER 1955

Closed November 15, 1955  
Issued December 15, 1955

## AN INVESTIGATION OF CYCLONE DEVELOPMENT— STORM OF DECEMBER 13-15, 1951

LYNN L. MEANS<sup>1</sup>

U. S. Weather Bureau, Chicago, Ill.

in collaboration with the

Weather Forecasting Research Center,<sup>2</sup> Department of Meteorology, University of Chicago

[Manuscript received February 21, 1955; revised September 9, 1955]

### ABSTRACT

The development of a storm which occurred in the United States during the period December 13-15, 1951 is investigated. An attempt is made to ascertain to what extent this development could be accounted for by the terms in the vorticity equation which derive from the vorticity advection and the thermal advection. It is found that the computed patterns agree well with those observed, although the numerical values are considerably exaggerated. Computed values of vertical velocity and divergence are compared with the observed patterns of clear sky and precipitation, and, on the whole, good agreement is found. The findings have gained further support from other storm studies and from experience in the use of vorticity charts and thermal advection charts in routine forecasting.

### CONTENTS

	Page
Abstract.....	185
1. Introduction.....	185
2. General synopsis.....	186
3. Test of a simplified hypothesis.....	188
4. Comparison of contributions by vorticity advection and thickness advection.....	190
5. Further discussion on observed development.....	192
6. Conclusions.....	196
Acknowledgments.....	197
Appendix—symbols and equations.....	197
References.....	198

### 1. INTRODUCTION

The present investigation forms a part of a program for studying cyclone development in the lower troposphere and deals with the fourth storm (Dec. 13-15, 1951) in this series chosen for a detailed fact-finding diagnostic study of development. The program which has been conducted jointly by the Weather Forecasting Research Center and the U. S. Weather Bureau District Forecast Center, Chicago, has been under the general direction of Prof. S. Petterssen. The general approach to and the theory underlying these investigations have been described in earlier papers (Petterssen [1], and Petterssen, Dunn, and Means [2]). For the convenience of the reader in interpreting terminology, symbols, and basic equations to be used in the sections that follow, these items from Petterssen's [1] theory of development are reproduced in the Appendix. In accordance with the general program, attempts have been made to compute vertical velocities, divergence, thermal advection, and vorticity changes. For a description of the methods of computation and the accuracies involved reference is made to an appendix to a report by Petterssen and Bradbury [3].

<sup>1</sup> Present address: National Weather Analysis Center, U. S. Weather Bureau, Washington, D. C.

<sup>2</sup> The research reported in this paper has been sponsored by the Geophysics Research Directorate of the U. S. Air Force Cambridge Research Center under contract No. AF 19(604)-309. It is published for technical information only, and does not necessarily represent recommendations or conclusions of the sponsoring agency.

## 2. GENERAL SYNOPSIS

The storm of December 13–15, 1951, was one of those moderate winter developments which in retrospect appear fairly routine, but which (as the writer can personally testify) offered real problems to the forecaster with reference to formation, movement, and increase in intensity, and also in related forecasts of precipitation, temperature, and wind. The following brief narrative of synoptic events during the development of this storm will provide the reader with some background for the more detailed analysis that follows. Charts illustrating the synoptic sequence are given in figures 1–3.

On December 12, 1951, a sea level pressure trough lay along the eastern slopes of the Rockies from Montana to western Texas (fig. 1a). On the 13th (fig. 1b) a center of low pressure was gradually organized in the northeastern corner of New Mexico as a fresh surge of polar air pushed south-southeastward along the eastern slopes through portions of Montana and Wyoming into Colorado. By 0300 GMT on the 14th (fig. 2a) the Low had begun to move eastward.

As the Low moved toward the lower Mississippi Valley a precipitation shield gradually developed and soon extended as far as 600 miles north and east from the center. During the day on the 14th a narrow band of heavy snow formed about 300 miles north of the low center, stretching from southeastern Nebraska across southern Iowa and extreme northern Illinois into southern Lower Michigan. Rainfall amounts of  $\frac{1}{4}$  to  $\frac{1}{2}$  inch in 6 hours developed early on the 14th over Arkansas. The forward edge of this area of moderate to heavy rainfall moved rapidly up the Ohio Valley staying about 12 hours distance ahead of the movement of the sea level Low.

The circulation around the low center intensified considerably, especially after 1500 GMT, December 14 (fig. 2b) although the central pressure had dropped a maximum of only 10 mb. from 0300 GMT, December 14 to 0300 GMT, December 15 (fig. 3a). However this intensification did not continue long. As the Low moved into Pennsylvania on the 15th, a secondary wave formed off the New Jersey coast. Such a secondary formation is not infrequent. This secondary wave became the primary center by 1500 GMT December 15 (fig. 3b) as the cyclonic circulations merged off the New England coast.

At 500 mb. the broadscale pattern for the same synoptic sequence featured at 1500 GMT, December 12, a major trough over eastern Canada and the eastern United States, and a major ridge off the Pacific coast. This large amplitude ridge extended northwestward to the Bering Sea with strong winds and sharp anticyclonic curvature at the crest of the ridge. An important area of height falls formed in the current downstream from this ridge. The movement southeastward of this area of height falls into the col separating the Low off the southern California coast (fig. 1a) from the main current of the westerlies, opened up the closed Low so that by 1500 GMT on the 13th

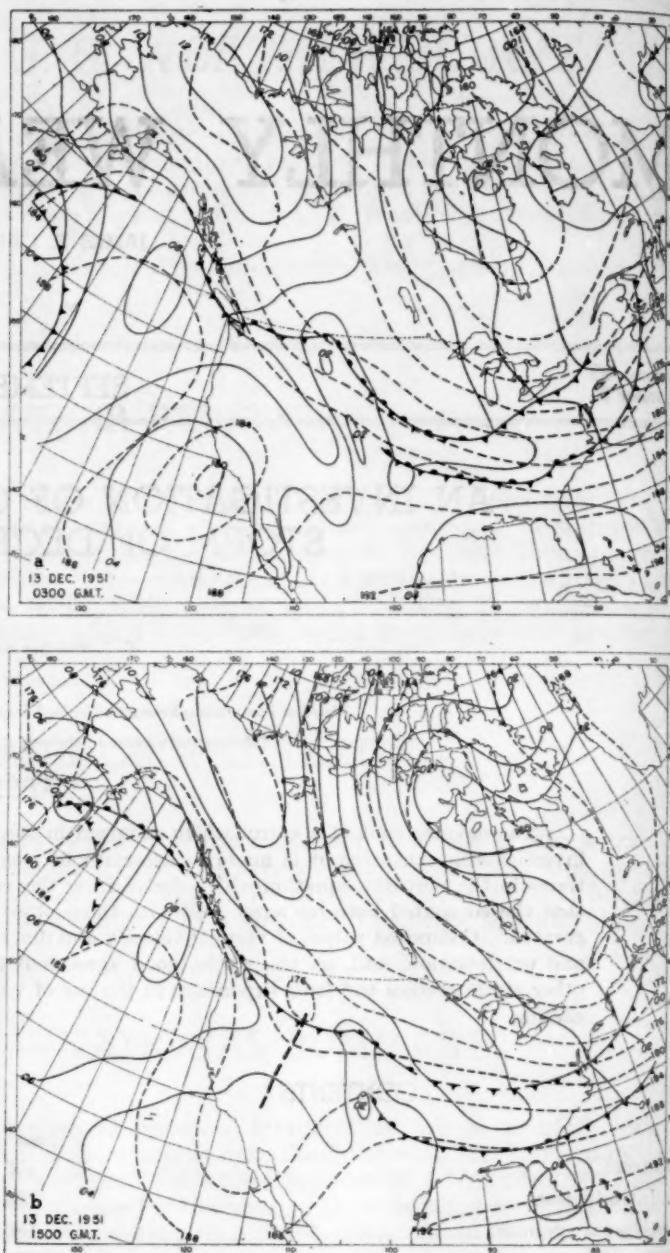


FIGURE 1.—Contours of 1000-mb. (solid lines) and 500-mb. (dashed lines) surfaces in hundreds of feet, and sea level fronts at 0300 and 1500 GMT, December 13, 1951.

(fig. 1b) it was rapidly becoming converted into an open trough.

The increase in amplitude of the trough downstream from the large amplitude ridge had now altered the picture over the southwestern United States considerably. On December 13 at 1500 GMT (fig. 1b) there was a minor trough over the northern Rockies as well as the nearly open trough just off the California coast which together, as we shall see later, formed a single area of positive vorticity advection at the 300-mb. level from Wyoming southward to New Mexico. It was at this time that the surface Low was becoming well-defined.

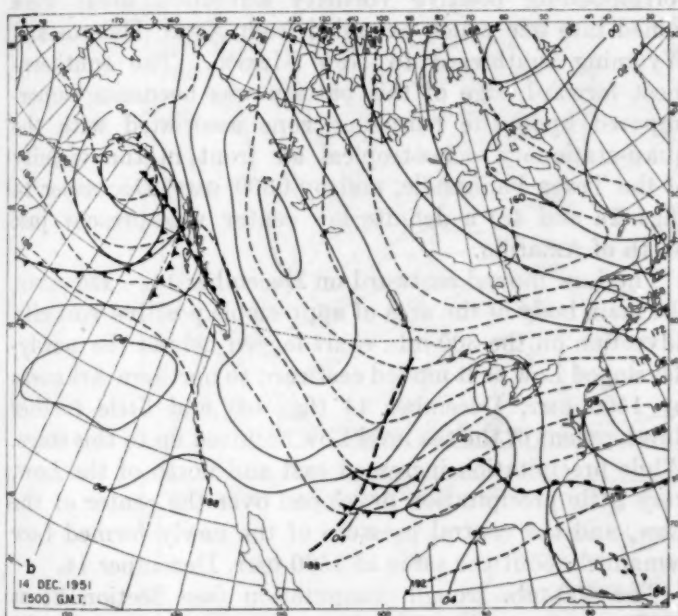
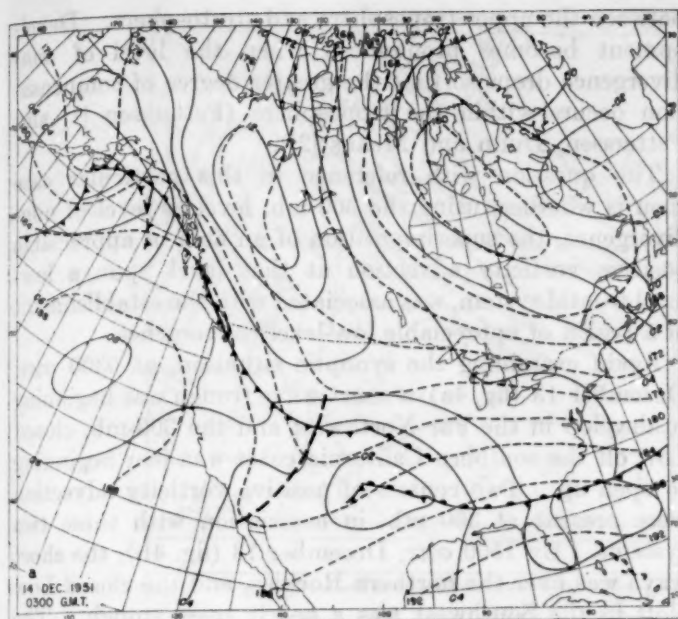


FIGURE 2.—Contours of 1000-mb. (solid lines) and 500-mb. (dashed lines) surfaces in hundreds of feet and sea level fronts at 0300 and 1500 GMT, December 14, 1951.

By December 14, 0300 GMT (fig. 2a) the 500-mb. short wave pattern over the Rocky Mountain and Plateau area, as represented by the contours and isallohypes, was consolidated into a single wave which was obviously moving eastward in the main westerly current. Meanwhile strong rises in the contour heights were filling the trough over the eastern United States, and the broad flow pattern was tipping from mainly northwesterly flow over the central United States at 0300 GMT December 13 to mainly southwesterly at 1500 GMT December 14 (fig. 2b). The surface Low intensified under this southwesterly flow aloft.

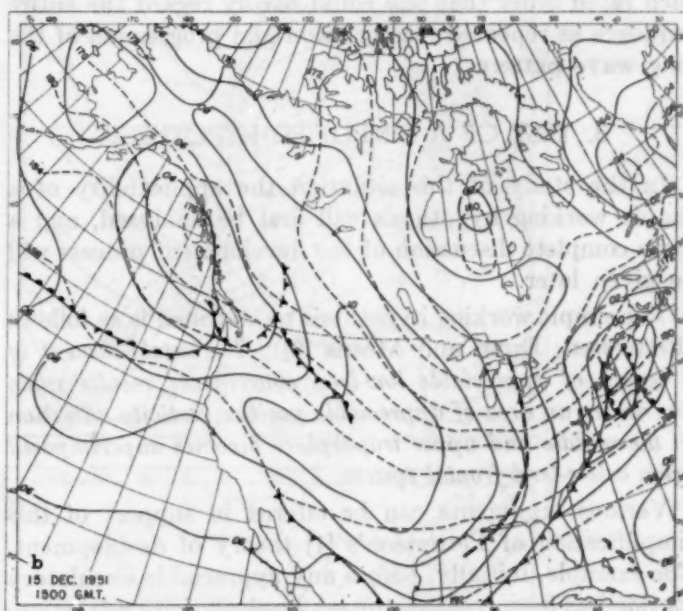
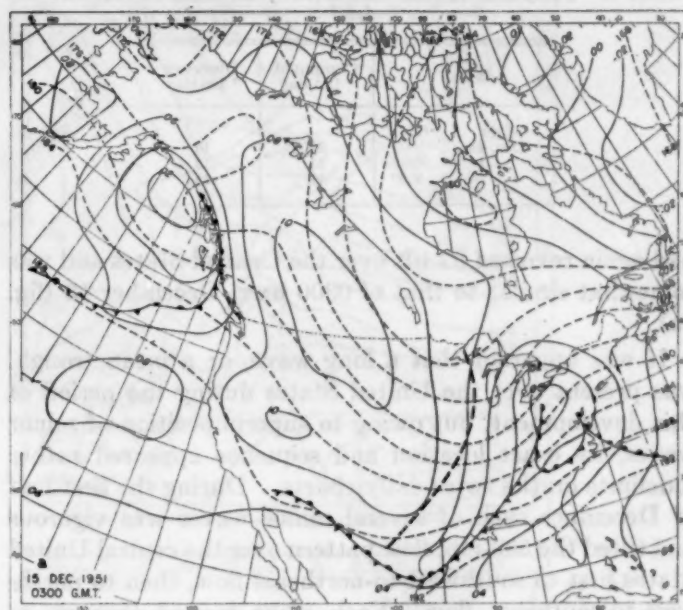


FIGURE 3.—Contours of 1000-mb. (solid lines) and 500-mb. (dashed lines) surfaces in hundreds of feet, and sea level fronts at 0300 and 1500 GMT, December 15, 1951.

The 500-mb. trough also intensified as it moved eastward across the United States. This intensification is consistent with the northeast to southwest tilt (fig. 2a) of the trough (Petterssen [4]) although other processes may have contributed also.

Computations by the aid of Petterssen's wave formula (Petterssen [4]) for 24-hour movements of the trough at the 500-mb. level are given in table 1.

By 0300 GMT, December 16, the major trough was again found over the Atlantic Coast States as it had been before this storm developed, and the main current at 500 mb.

TABLE 1.—Computed 24-hour movement of the trough at the 500-mb. level

Time		Computed ° Lat/day	Observed ° Lat/day
Date	GMT		
Dec. 13	1500	10	10
14	0300	11	13
14	1500	11	13

had again reversed its tilt over the Central States and was somewhat similar to that of 0300 GMT, December 13 (fig. 1a).

It was apparent that a long wave, or a mean trough, was present over the United States during the period of this development, but owing to superimposition of minor waves, its exact location and sequence appeared rather indefinite on the twice-daily charts. During the first half of December each of several minor waves was vigorous and tilted the 500-mb. flow pattern over the central United States first to southwest-to-northeast flow, then to northwest-to-southeast flow. Each wave moved through in such rapid order that one could hardly regard the entire sequence as repeated retrogression and progression of the long wave pattern.

### 3. TEST OF A SIMPLIFIED HYPOTHESIS

In the study of this situation the applicability of a simple working hypothesis will first be analyzed, and a more complete discussion of the development process will be given later.

The simple working hypothesis to be tested is as follows (Petterssen, Dunn and Means [2]): *The establishment of a region of appreciable low-level convergence results when and where an area of appreciable positive vorticity advection in the middle and upper troposphere becomes superimposed upon a low-level frontal system.*

Various arguments can be offered in support of this simplification of Petterssen's [1] theory of development. For example, initially, before any appreciable circulatory motion has been created, the sea level vorticity advection, the Laplacian of the thermal advection, and the vertical velocity-stability terms are likely to be small in the vicinity of the center of the weak surface Low. Neglecting these terms and the non-adiabatic term, equation (2.5) (Appendix) reduces to  $D_0 Q_0 = -A_{QL}$  where  $A_{QL}$  is the vorticity advection at the level of non-divergence, and  $D_0$  and  $Q_0$  are the divergence and the absolute vorticity (vertical component) at sea level. Since  $Q_0$  remains positive,  $A_{QL}$  gives a qualitative indication of convergence at sea level.

Since Petterssen's approach to the development problem deals with the level of nondivergence and the layer between that level and sea level, a primary consideration in the testing of this hypothesis is the height of the level of nondivergence. In typical cases the level of nondivergence is in the upper troposphere or near the tropopause before and during the early stages of development. The compensation in the divergence field is then primarily

between the upper troposphere and stratosphere. Development becomes pronounced when the level of nondivergence drops so that the greater degree of compensation occurs within the troposphere (Petterssen [1] and Petterssen, Dunn and Means [2]).

The question with reference to this particular case then is whether, using the 300-mb. level as level of nondivergence, the superimposition of an area of appreciable positive vorticity advection at that level upon a low-level frontal system, was associated with the establishment of a region of appreciable low-level convergence.

Again examining the synoptic situation, at 0300 GMT, December 13 (fig. 4a), a short-wave trough was beginning to develop in the Far Northwest and the 300-mb. closed Low off the southern California coast was just beginning to open up. Two centers of positive vorticity advection were present at 300 mb. in association with these two systems. By 1500 GMT, December 13 (fig. 4b), the short wave was over the northern Rockies, and the closed Low aloft in the Southwest was a nearly open trough. The corresponding positive vorticity advection areas were joined into one which extended from North Dakota and Wyoming southward to New Mexico. The southernmost forward edge of this pattern was becoming superimposed upon the baroclinic zone associated with the quasi-stationary polar-tropical air front in the vicinity of the Texas Panhandle, and by 0300 GMT, December 14 (figs. 2a and 4c) a definite low center was present just north of Amarillo.

The Low moved eastward on December 14. However, the main body of the area of appreciable positive vorticity advection on the 300-mb. chart lagged behind the newly-developed Low as it moved eastward to northern Arkansas by 1500 GMT, December 14 (fig. 4d) and little further development of the sea level Low occurred up to this stage. While precipitation increased east and north of the Low, very little precipitation developed over the center of the Low, and the central pressure of the newly formed Low remained about the same at 1500 GMT, December 14.

The 500-mb. trough computation (see Section 2) at 0300 GMT, December 14 indicated that the trough should continue moving eastward at a moderate speed, possibly with some acceleration. The vorticity advection at the 500- and 300-mb. levels showed a very marked increase over the center of the Low between 1500 GMT on the 14th and 0300 GMT on the 15th (fig. 4d and e). This was associated with (1) a decrease in central pressure, and increased circulation around the Low (fig. 3a); (2) a lowering of the level of nondivergence (as will be shown later, fig. 6) from about 400 mb. to 600 mb.; and (3) a marked increase in the area and amounts of precipitation in the vicinity of the center of the Low. (All of these occurred between 1500 GMT on the 14th and 0300 GMT on the 15th.)

Vorticity advection amounts for 500 and 300 mb. were still strong but decreasing over the low center at 1500 GMT, December 15 (fig. 4f).

This case then showed general agreement with the simplified hypothesis and with the typical sequence of

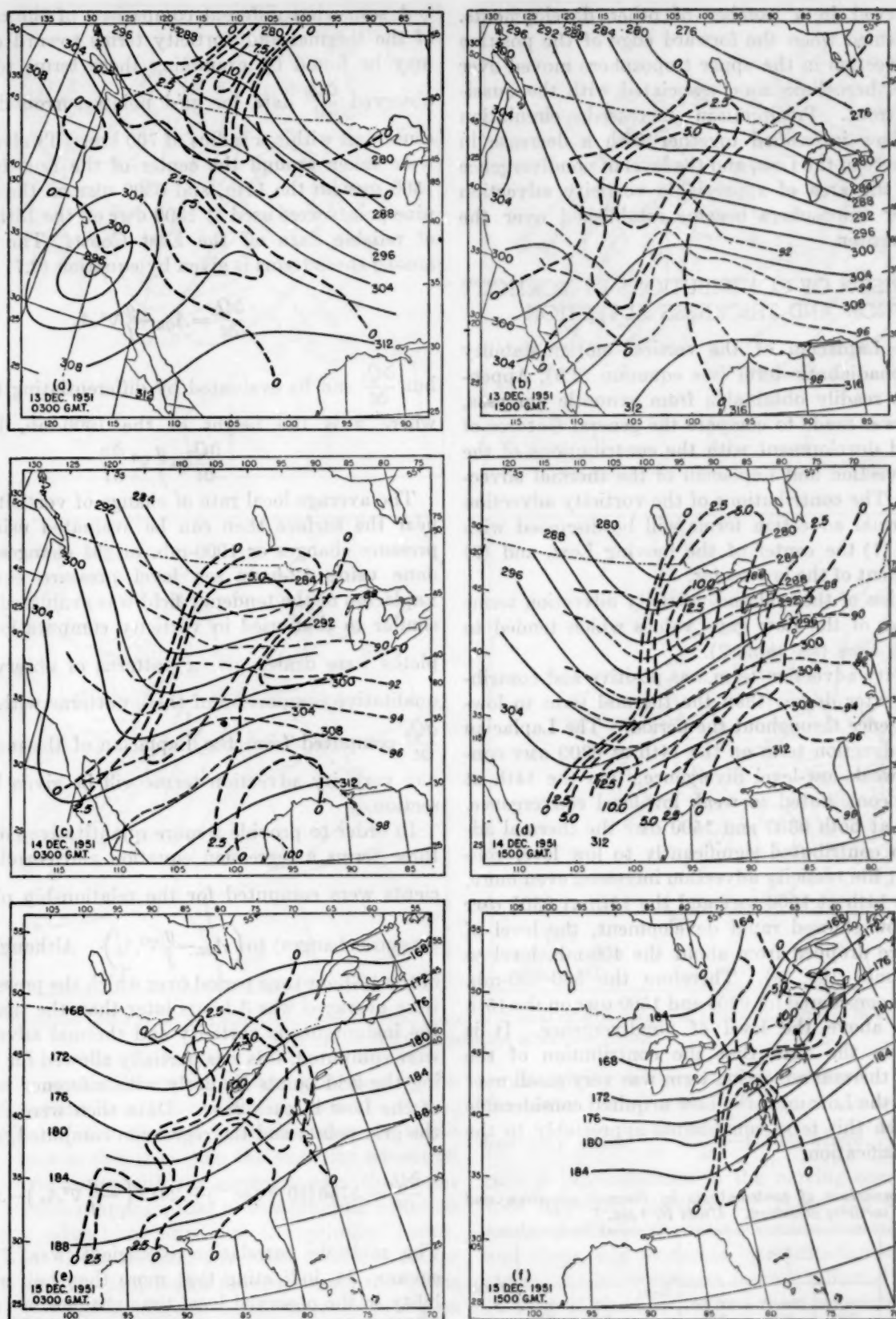


FIGURE 4.—(a-d) Contours of 300-mb. surface (solid lines) and thickness 1000-700 mb. (light broken lines) in hundreds of feet, and vorticity advection (heavy broken lines) at 300 mb. in units of  $10^{-3} \text{ sec.}^{-2}$ . (e-f) Dot represents surface center. (e-f) 500-mb. contours (solid lines) and vorticity advection (broken lines) 0300 and 1500 GMT, December 13, 14, 15, 1951.

events observed in a number of other developments. The Low formed when the forward edge of the positive vorticity advection in the upper troposphere moved over the low-level baroclinic zone associated with the quasi-stationary front. Precipitation increased, circulation about the Low intensified together with a decrease in central pressure of the Low, and the level of nondivergence dropped as the area of appreciable vorticity advection in the upper troposphere became established over the surface low center.

#### 4. COMPARISON OF CONTRIBUTIONS BY VORTICITY ADVECTION AND THICKNESS ADVECTION

Since the Laplacian of the vertical motion-stability term and nonadiabatic term (see equation (2.6), Appendix) are not readily obtainable from synoptic analyses, an attempt was made to compare the general features of the observed development with the contributions of the vorticity advection and Laplacian of the thermal advection terms. The contributions of the vorticity advection and the thermal advection terms will be discussed with reference to (1) the center of the moving Low, and (2) the environment of the low center.

Computation of thermal and vorticity advection terms over the center of the Low gave values which tended to increase with time (see table 2).

The vorticity advection term was positive and contributed to a greater degree than the thermal term to low-level convergence throughout the period. The Laplacian of thermal advection term on the 14th at 0300 GMT contributed to weak low-level divergence. On the 14th at 1500 GMT it contributed to weak low-level convergence. On the 15th at both 0300 and 1500 GMT the thermal advection term contributed significantly to low level convergence, but the vorticity advection increased even more. Between the 14th at 1500 GMT and the 15th at 0300 GMT when the Low showed rapid development, the level of nondivergence dropped from about the 400-mb. level to about 600 mb. (fig. 6). Therefore the 500-300-mb. layer was not considered for 0300 and 1500 GMT on the 15th as this was above the level of nondivergence. It is apparent from the data that the contribution of the Laplacian of thermal advection term was very small over the center of the Low until the Low acquired considerable intensity; then this term contributed appreciably to the further intensification.

TABLE 2.—Comparison of contributions by thermal advection and vorticity advection. Units  $10^{-9}$  sec.<sup>-2</sup>

Time		$-\frac{g}{f}\nabla^2 A_h$			Sum for layer	$A_{QL}$		Total
		1000-700 mb.	700-500 mb.	500-300 mb.		500 mb.	300 mb.	
Date	GMT							
Dec. 14	0300	-.3	-1.8	1.7	-0.4		3.5	3.1
14	1500	-.1	1.6	-0.9	.6		2.0	2.6
15	0300	.8	3.3		4.1	8.0		12.1
15	1500	3.8	1.6		5.4	7.0		12.4

A somewhat different comparison of the contributions of the thermal and vorticity terms toward development may be found by examining those terms together with observed  $\frac{\partial Q_0}{\partial t}$  data for grid points surrounding the low center, all within a radius of 700 km. Twelve grid points were taken around the center of the Low for 0300 and 1500 GMT on the 14th, and 0300 GMT on the 15th. Only nine points were used at 1500 GMT on the 15th due to lack of reliable data off the East Coast. The relationship among these terms is given by equation (2.7) (Appendix):

$$\frac{\partial Q_0}{\partial t} = A_{QL} - \frac{g}{f} \nabla^2 A_h$$

but  $\frac{\partial Q_0}{\partial t}$  can be evaluated by differentiating  $Q_0 = \frac{g}{f} \nabla^2 z + f$  where  $z$  is the height of the 1000-mb. level. Thus

$$\frac{\partial Q_0}{\partial t} = \frac{g}{f} \nabla^2 \frac{\partial z}{\partial t}$$

The average local rate of change of vorticity with time near the surface then can be evaluated using sea level pressure changes or 1000-mb. height changes. This was done using 12-hour sea level pressure changes. The Laplacian of the tendency field was evaluated from a grid similar to that used in vorticity computations, and isopleths were drawn giving patterns of observed  $\frac{\partial Q_0}{\partial t}$ . A qualitative comparison of these patterns with patterns of  $\frac{\partial Q_0}{\partial t}$  computed from the Laplacian of thermal advection and vorticity advection terms will be given later in this section.

In order to provide a more quantitative comparison of these terms a regression equation and correlation coefficients were computed for the relationship of  $\frac{\partial Q_0}{\partial t}$  (from pressure changes) to  $(A_{QL} - \frac{g}{f} \nabla^2 A_h)$ . Although the center of the 12-hour time period over which the pressure changes were averaged was 3 hours later than the time for which the instantaneous vorticity and thermal advection terms were computed, this was partially allowed for by positioning the grid points similarly with reference to the center of the Low in each case. Data then were extracted for the grid points and the regression computed, giving:

$$\frac{\partial Q_0}{\partial t} = .3756 (10^{-9} \text{ sec}^{-2}) + .2012 \left( -\frac{g}{f} \nabla^2 A_h \right) - .0144 (A_{QL})$$

The multiple correlation coefficient was .74, with its square, .54, indicating that more than half of the variability in the observed local time changes in vorticity was accounted for. The correlation of the local time change of vorticity with the Laplacian of thermal advection term alone was .736 and the correlation with the vorticity advection term alone was .24, and partial correlation coefficients were .72 and .02.

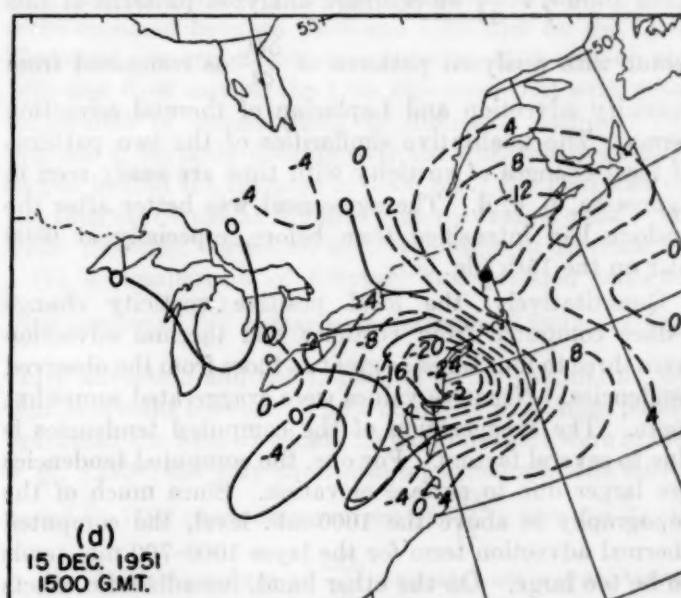
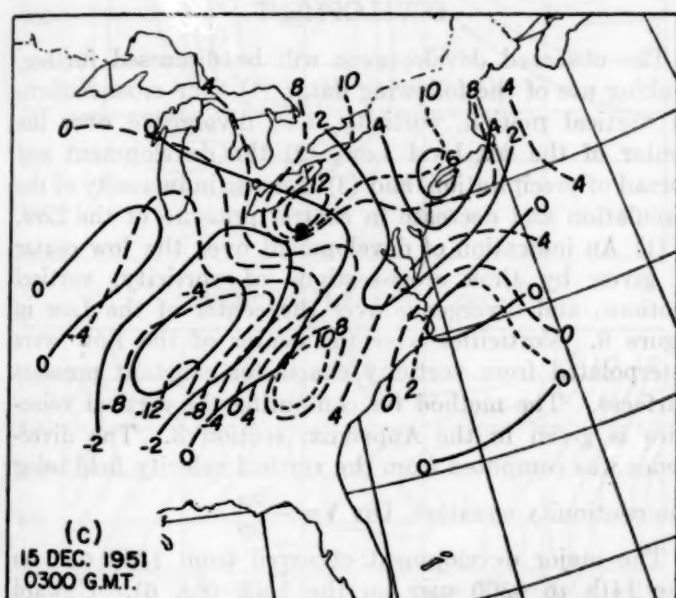
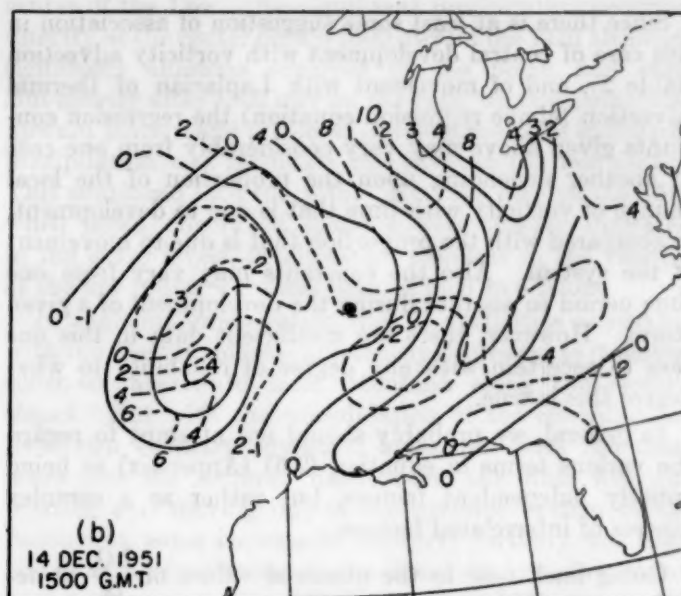
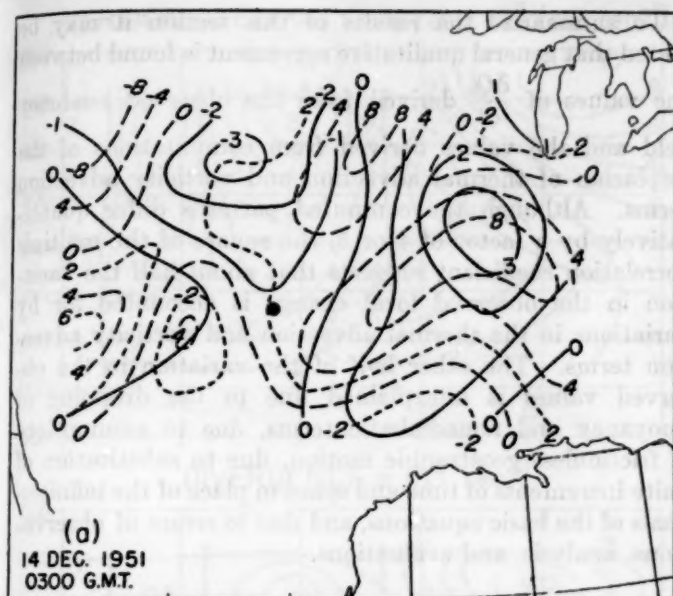


FIGURE 5.—Observed (solid lines) and computed (broken lines) patterns of local rate of change of 1000-mb. vorticity in units of  $10^{-4}$  sec.<sup>-2</sup>. Large dot indicates position of surface center.

The above correlation coefficients suggest that in the environment of the Low, but not directly over the center, the Laplacian of the thermal advection appears to be more important in this case than the vorticity advection term. This contrasts with the situation over the center of the Low where it appears that in this synoptic situation the vorticity advection term was the primary factor. The Laplacian of the thermal advection term was rather large when the Low first began moving across the Texas Panhandle, but the significant amounts contributing to low-level divergence were to the rear of the Low, and significant amounts contributing to low-level convergence were in advance of the Low. These significant values of the Laplacian of thermal advection term straddled the

center giving little net contribution in the vicinity of the center. If  $\mathbf{C}$  is the velocity of the sea level system one may write  $\frac{\partial Q_0}{\partial t} = \frac{\delta Q_0}{\delta t} - \mathbf{C} \cdot \nabla Q_0$  where  $\frac{\delta Q_0}{\delta t}$  is the local rate of intensification in the moving coordinate system. (See Appendix, section 2.) Since the local change is made up of both the intensification and convective terms, and since only moderate intensification occurred in this storm, the local changes largely reflected the movement ( $\mathbf{C} \cdot \nabla Q_0$ ) of the Low. Since the Laplacian of the thermal advection term was predominant for areas away from the center as indicated by the regression and correlation coefficients, this term probably was associated mostly with movement of the Low.

Since there is at least some suggestion of association in this case of central development with vorticity advection (table 2), and of movement with Laplacian of thermal advection (above regression equation) the regression constants given above may vary considerably from one case to another depending upon the proportion of the local change of vorticity with time that is due to development, as compared with the proportion that is due to movement of the system. Also the constants may vary from one time period to another during the development of a given storm. However, there are insufficient data in this one case to ascertain with any degree of reliability to what degree this is true.

In general, we probably should not attempt to regard the various terms in equation (2.6) (Appendix) as being entirely independent factors, but rather as a complex process of interrelated factors.

Going back now to the observed values of  $\frac{\partial Q_0}{\partial t}$  as derived from  $\frac{g}{f} \nabla^2 \frac{\partial z}{\partial t}$  we compare analyzed patterns of this factor with analyzed patterns of  $\frac{\partial Q_0}{\partial t}$  as computed from vorticity advection and Laplacian of thermal advection terms. The qualitative similarities of the two patterns of local changes of vorticity with time are easily seen in figures 5a, b, c, d. The agreement was better after the cyclone had intensified than before, especially at 0300 GMT on the 15th (fig. 5c).

Quantitatively, the local positive vorticity change values computed from vorticity and thermal advection were three to four times as great as those from the observed tendencies. Negative values were exaggerated somewhat more. The exaggeration of the computed tendencies is due to several factors. For one, the computed tendencies are larger due to surface elevation. Since much of the topography is above the 1000-mb. level, the computed thermal advection term for the layer 1000-700 mb. tends to be too large. On the other hand, nonadiabatic effects tend to counteract thermal advection. The vertical motion-stability,  $\omega(\Gamma_a - \Gamma)$  term which was also neglected, usually tends to act as a brake except, of course, when  $\Gamma > \Gamma_a$ , which may occur briefly over somewhat limited portions of the cyclonic system. Therefore omission of this term could cause computed changes to be too large. An appreciable portion of the error may be due to the geostrophic assumption and to frictional forces which would also cause the computed changes to be too large. Computed negative values were especially exaggerated as compared with observed. This is what we would expect since ascending motion is largely wet-adiabatic while downward motion is largely dry-adiabatic. The omission of the buoyancy term, then, tends to exaggerate the computed negative vorticity changes more than the positive vorticity changes.

In general the vorticity transport terms were greater above 500 mb. and the Laplacian of thermal advection terms were greater below 500 mb.

To summarize the results of this section it may be stated that general qualitative agreement is found between the values of  $\frac{\partial Q_0}{\partial t}$  derived from the observed tendency field and the values derived from computations of the Laplacian of thermal advection and vorticity advection terms. Although the computed patterns differ quantitatively by a factor of 4 or 5, the square of the multiple correlation coefficient suggests that about half the variation in the observed local change is accounted for by variations in the thermal advection and vorticity advection terms. The other half of the variation in the observed values is unexplained due to the dropping of buoyancy and nonadiabatic terms, due to assumptions of frictionless geostrophic motion, due to substitution of finite increments of time and space in place of the infinitesimals of the basic equations, and due to errors of observations, analysis, and evaluations.

## 5. FURTHER DISCUSSION ON OBSERVED DEVELOPMENT

The observed development will be discussed further, making use of the following data: (1) time cross-sections of vertical motion, vorticity, and divergence over the center of the sea level Low, (2) the development and spread of precipitation, and (3) increase in intensity of the circulation and decrease in central pressure of the Low.

(1) An indication of development over the low center is given by time cross-sections of vorticity, vertical motions, and divergence over the center of the Low in figure 6. Vorticities over the center of the Low were interpolated from vorticity charts for constant pressure surfaces. The method for computing the vertical velocities is given in the Appendix, section 3. The divergence was computed from the vertical velocity field using the continuity equation,  $\text{Div } \mathbf{V} = -\frac{\partial \omega}{\partial p}$ .

The major development occurred from 1500 GMT on the 14th to 0300 GMT on the 15th (fig. 6). Upward velocities and low-level convergence were greatest at 1500 GMT on the 14th. The level of nondivergence, as indicated by the heavy solid line, dropped rapidly during that period from about the 400-mb. level to about the 600-mb. level at 0300 GMT on the 15th. The sudden "flareup" of development was preceded by weak upward motion at the 850-mb. level at 0300 GMT on the 14th when the Low was just beginning to move away from its place of formation. Downward motion, which was especially marked at the 300- and 500-mb. levels at this time, was probably associated with flow across the mountains which were close by to the west. Following the flareup mean downward motion developed at 1500 GMT on the 15th throughout the air column over the low center, although some low-level convergence persisted. These patterns were weak in the lower troposphere, but divergence and downward motion were strong in the upper troposphere. This was consistent with the fact that by this time the original Low was beginning to fill

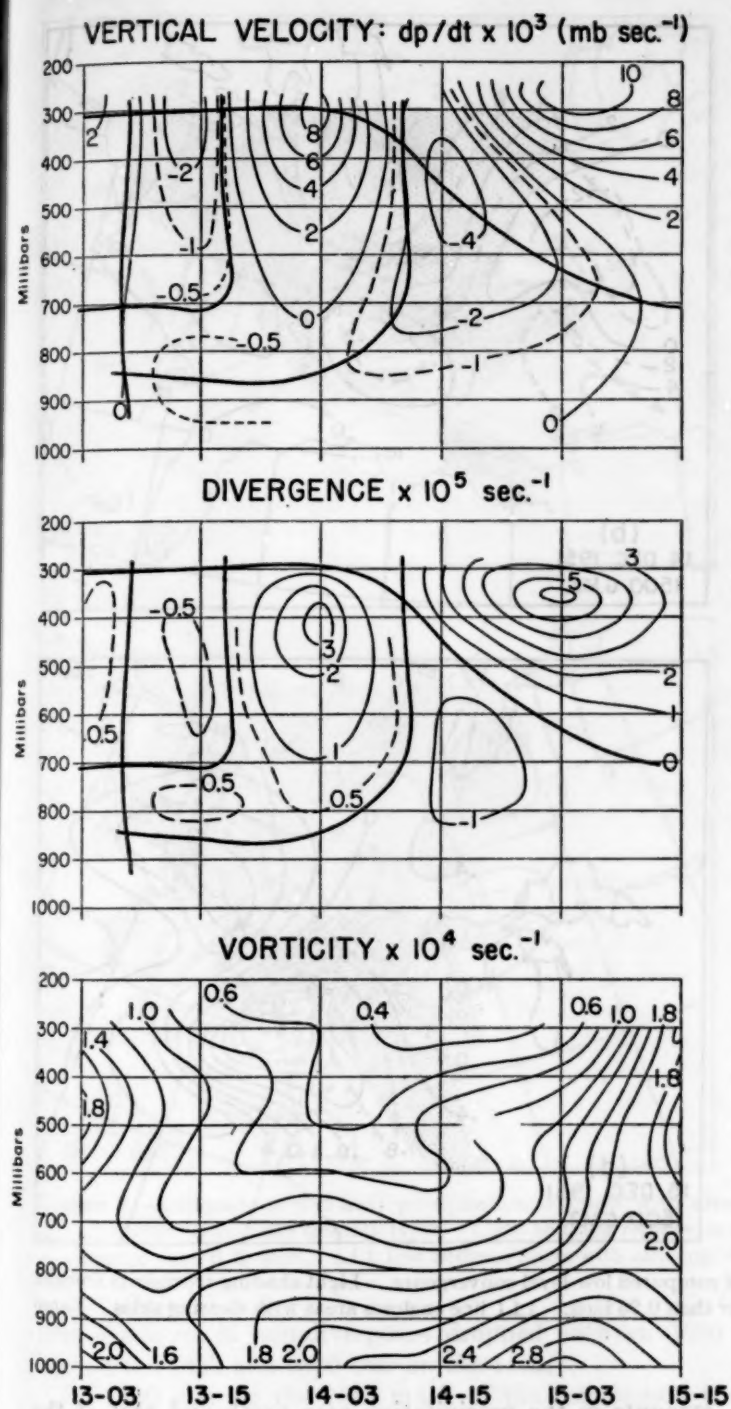


FIGURE 6.—Distribution of absolute vorticity, divergence, and vertical velocity in the column over the sea level center for the period December 13–15, 1951.

as a deepening secondary wave off the coast of Maine became the principal center. This was the secondary that had been forming off the New Jersey coast as the original Low moved into Pennsylvania.

These vertical motions and indications of convergence and divergence (fig. 6) over the center of the Low were consistent with the occurrence of precipitation at the

center of the Low. No significant precipitation occurred directly at the center before 1500 GMT on the 14th although significant amounts occurred to the north and east. But shortly after 1500 GMT on the 14th, when considerable upward motion and low-level convergence were indicated, precipitation was moderate to heavy at the low center. This continued into the 15th. By 1500 GMT on the 15th when mean downward motions were weakly indicated in the lower levels, precipitation amounts in the vicinity of the low center were less than  $\frac{1}{8}$  inch in 6 hours.

In the time cross-section (fig. 6) vorticities associated with the moving impulse apparently decreased as it moved south-southeastward from Montana along the eastern slopes. But with the consolidation of the contributions from two vorticity advection areas, one with the short wave over the northern Rockies and the other with the opening and moving out of the cyclonic system in the Southwest, some increase in low-level vorticity was associated with organization of the closed sea level low center over northeastern New Mexico between 1500 GMT on the 13th and 0300 GMT on the 14th. Little further development occurred between 0300 and 1500 GMT on the 14th. The most important increase, between 1500 GMT on the 14th and 0300 GMT on the 15th was consistent with other indications of development as discussed earlier. The increase in vorticity directly over the 1000-mb. low center lagged behind the increase at 1000 mb. By 1500 GMT on the 15th vorticities at 300 mb. were reaching a peak value while 1000-mb. vorticities were beginning to decrease.

(2) A comparison of 6-hourly precipitation patterns with computed  $\frac{\partial Q_0}{\partial t}$  patterns as determined from the vorticity advection and the Laplacian of the thermal advection, is of some interest. The 6-hourly precipitation period bracketed the time at which the computations were made, e. g., 1230–1830 GMT precipitation accumulations correspond to 1500 GMT computations of  $\frac{\partial Q_0}{\partial t}$ . (See fig. 7a, b, c, d). Positive values of  $\frac{\partial Q_0}{\partial t}$  give at least a qualitative

indication of low-level convergence, and negative values, low-level divergence. Two categories of 6-hourly precipitation are outlined: less than .25 inch, and .25 inch and more. Smaller amounts of precipitation, usually less than .10 inch, were frequently associated with orographic effects or low-level instability and stratocumulus clouds where cold air was flowing over warmer ground or over the warmer waters of the Great Lakes, and some of these small precipitation amounts occurred locally despite indications of computed low-level divergence. Areas of clear skies or scattered to broken low clouds are also indicated in figure 7 and may be compared with areas of computed low-level divergence.

Some of the precipitation indicated at 0300 GMT on the 14th (fig. 7a) along the eastern slopes of the Rockies was undoubtedly associated with orographic lifting in the east to northeast winds at low levels over that area especially since it ended rapidly as winds shifted to a downslope

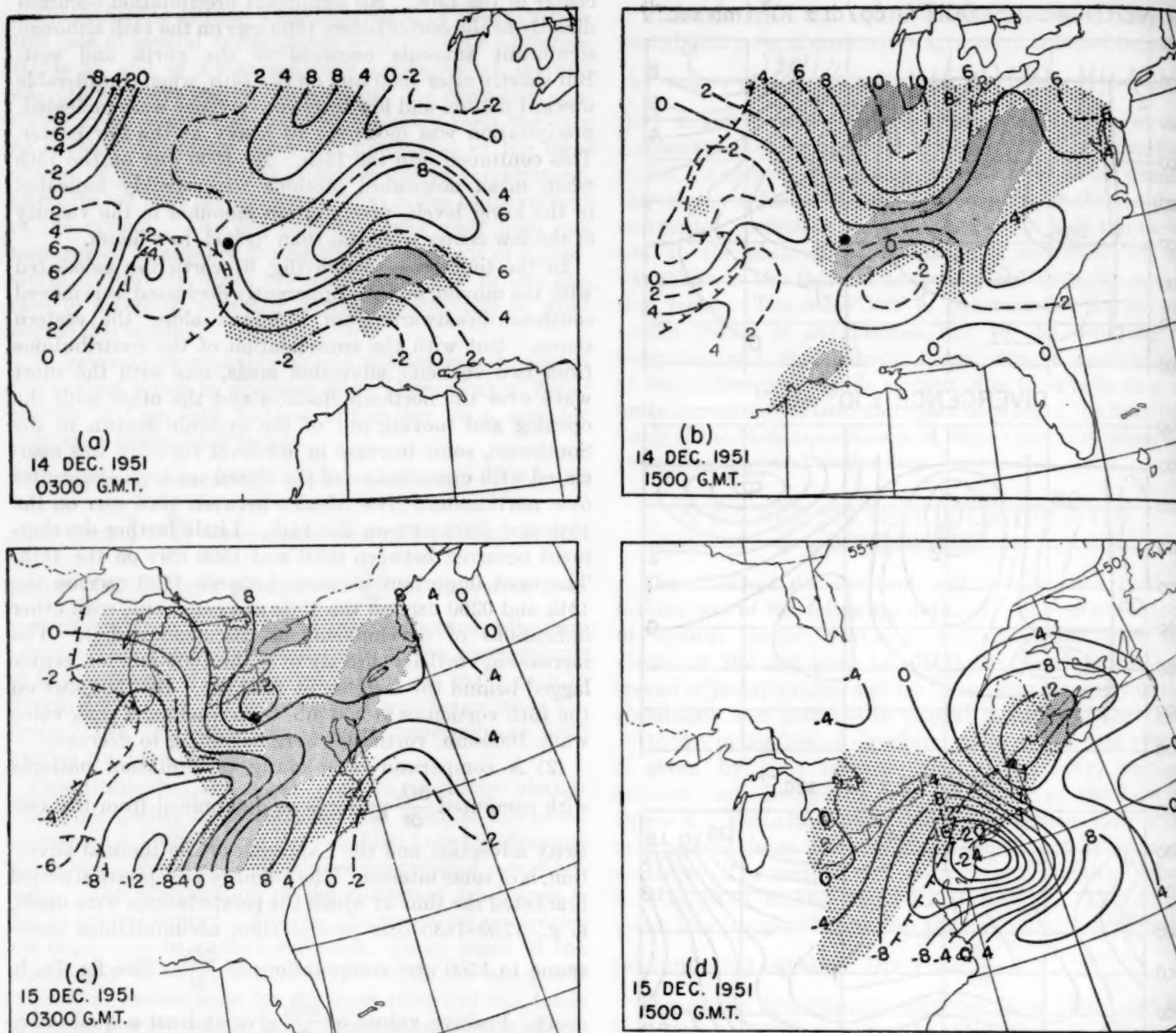


FIGURE 7.—Comparison of 6-hour precipitation amounts with areas of computed low-level convergence. Light shading represents amount less than 0.25 inch and heavy shading, amounts equal to or greater than 0.25 inch. --- line encloses areas with clearing skies. Large dot indicates position of surface center.

component. Really significant amounts of rainfall were developing at this time over Arkansas along the southern edge of a computed area of low-level convergence. The heavier amounts of precipitation continued to be associated through the period of this development with the southern portion of the area of low-level convergence. Warmer and more moist air was present in the lower layers in that portion of the convergence area. This emphasizes the importance of moisture content of the air and probably also its degree of stability.

The Laplacian of the thermal advection amounts were larger in the area ahead of the Low than at the low center. They were also usually larger than the vorticity advection

amounts in the precipitation area north and east of the storm center.

An interesting feature of the chart for 1500 GMT, December 14 (fig. 7b) is the isolated area of heavier precipitation southwest of the southern tip of Lake Michigan, which suggests that the flow of cold air in the east to northeast surface winds across the relatively warm Lake waters contributed locally to increased precipitation amounts. An accumulation of 10 inches of snow was reported at Chicago.

The layer 1000–300 mb. is used for comparison at 0300 and 1500 GMT on the 14th while the layer 1000–500 mb. is used at 0300 and 1500 GMT on the 15th due to the fact

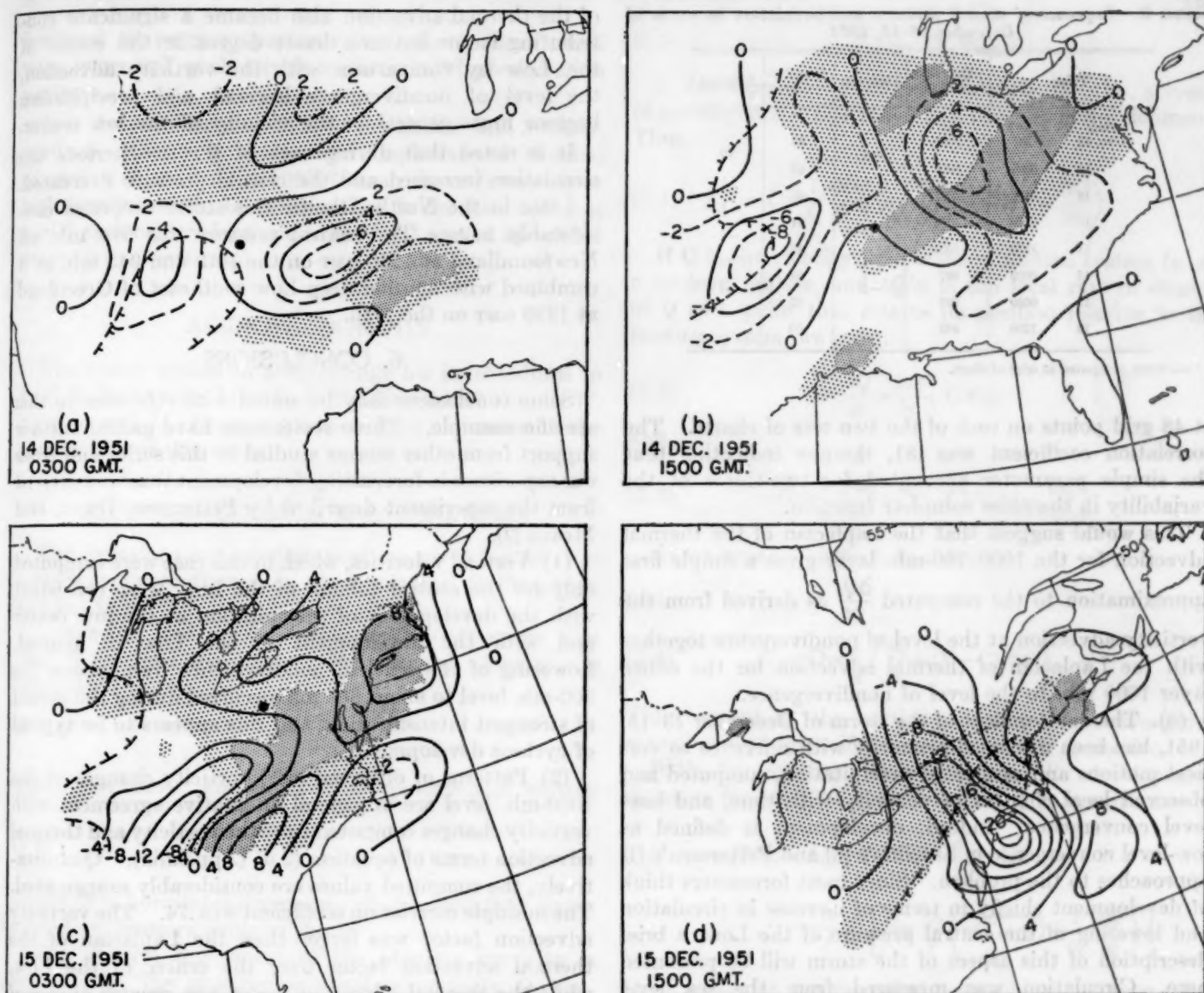


FIGURE 8.—Comparison of 6-hour precipitation amounts with areas of low-level convergence as computed from Laplacian of thermal advection term, 1000-700-mb. layer. Light shading represents amounts less than 0.25 inch and heavy shading, amounts equal to or greater than 0.25 inch. 111 line encloses areas with clearing skies. Large dot indicates position of surface center.

that the level of non-divergence dropped between 1500 GMT on the 14th and 0300 GMT on the 15th.

By 1500 GMT on the 15th much of the comparison is lost because the main body of precipitation was moving off the northeast coast. Considerable snow flurry activity persisted between the Great Lakes and the Appalachians as is usually the case to the rear of such winter storms. Areas of computed low-level divergence were in general qualitative agreement with areas of clear or clearing skies, although in some areas stratocumulus clouds and even snow flurries tended to persist for a while to the rear of the development due to orographic and air mass modification factors.

In the analysis of these data, precipitation patterns appeared to be closely related to the Laplacian of the

thermal advection term,  $\left(-\frac{g}{f} \nabla^2 A_s\right)$ , especially that for the lower troposphere. (Appleby [5] has also found such a relation using forecast patterns of temperature advection at 850 mb.) Therefore a comparison was made between the 6-hourly precipitation and the Laplacian of the thermal advection patterns for the layer 1000-700 mb. This is shown in figure 8. General qualitative agreement is apparent in this case as was found in figure 7.

This was supported by a correlation between the simple  $\left(-\frac{g}{f} \nabla^2 A_s\right)_{1000-700}$  and the more elaborate values  $A_{QL}-\left(\frac{g}{f} \nabla^2 A_s\right)_{1000-300 \text{ or } 1000-500}$  upon which patterns in figure 8 and figure 7 are based respectively. Data were selected

TABLE 3.—Sequence of central pressure and circulation in storm of December 13–15, 1951

Time		Central pressure	Decrease	Circulation	Increase
Date	GMT	mb.			
Dec. 13	1230	1008		32	
14	0030	1000	-8	42	10
14	0630	1001	1	43	1
14	1230	1001	0	44	1
14	1830	1001	0	43	-1
15	0030	997	-4	58	15
15	0630	992	-5	57	-1
15	1230	992	0	( <sup>1</sup> )	

<sup>1</sup> No value computed at edge of chart.

at 48 grid points on *each* of the two sets of charts. The correlation coefficient was .81, thereby indicating that the simple parameter accounted for two-thirds of the variability in the more complete function.

This would suggest that the Laplacian of the thermal advection for the 1000–700-mb. layer gives a simple first approximation to the computed  $\frac{\partial Q_0}{\partial t}$  as derived from the vorticity advection at the level of nondivergence together with the Laplacian of thermal advection for the entire layer 1000 mb. to the level of nondivergence.

(3). The development of the storm of December 13–15, 1951, has been discussed primarily with reference to vertical motions and associated precipitation, computed and observed local changes of vorticity with time, and low-level convergence. Indeed, development is defined as low-level convergence in Sutcliffe's [6] and Petterssen's [1] approaches to the problem. Since most forecasters think of development chiefly in terms of increase in circulation and lowering of the central pressure of the Low, a brief description of this aspect of the storm will be presented here. Circulation was measured from the sea level charts using the technique outlined in Petterssen, Dunn, and Means [2]. Results are given in table 3.

These data show that the decrease in central pressure was more or less proportional to the increase in the circulation.

Two periods of intensification are evident. The first corresponds to the initial consolidation of a definite low center late on the 13th from a relatively unorganized trough along the lee slopes of the Rockies. Some vorticity advection was occurring at 300 mb. in the vicinity of the 1000-mb. low center during its initial development. It is believed that the southward movement of a cold High along the slopes of the Rockies also contributed to some increase in the computed circulation about the newly organized Low at this time.

The second period of development was that from 1830 GMT on the 14th to 0630 GMT on the 15th, which corresponds to the time period during which the vorticity advection increased considerably in the middle and upper troposphere in the vicinity of the low center, the Laplacian

of the thermal advection also became a significant contributing factor but to a lesser degree in the center of the Low by comparison with the vorticity advection, the level of nondivergence lowered, and precipitation became more general in the vicinity of the low center.

It is noted that during each of the two periods the circulation increased and the central pressure decreased.

Later in the North Atlantic this storm deepened considerably more. The central pressure was 974 mb. off Newfoundland at 1230 GMT on the 16th and 945 mb. as it combined with another deep Low southeast of Greenland at 1230 GMT on the 17th.

## 6. CONCLUSIONS

Some conclusions may be stated with reference to this specific example. These statements have gained further support from other storms studied in this series and from our experience in forecasting development that was derived from the experiment described by Petterssen, Dunn, and Means [2].

(1) Vertical velocities, which in this case were computed only for the central column of the Low, were consistent with the development of precipitation at the low center and with the development of the Low in general. Lowering of the level of nondivergence from above the 300-mb. level to about 600 mb. occurred during the period of strongest intensification, and this appears to be typical of cyclone development.

(2) Patterns of observed local vorticity changes at the 1000-mb. level are in general qualitative agreement with vorticity changes computed from the vorticity and thermal advection terms of equation (2.6) (Appendix). Quantitatively, the computed values are considerably exaggerated. The multiple correlation coefficient was .74. The vorticity advection factor was larger than the Laplacian of the thermal advection factor over the center of the Low, while the thermal advection factor was greater ahead of and to the rear of the moving Low.

(3) Low-level convergence patterns computed from the vorticity advection and thermal advection terms were in general qualitatively consistent with precipitation patterns. Precipitation amounts tended to be greater along the southern edge of the convergence patterns where more warm moist air was present in the lower layers, which emphasizes the importance of moisture content to the air and probably also its degree of stability.

(4) The development discussed in this report is consistent with the simplified hypothesis: "The establishment of a region of appreciable low-level convergence results when and where an area of appreciable vorticity advection in the middle and upper troposphere becomes superimposed upon a low-level frontal system."

(5) The joining of two areas of vorticity advection appeared to contribute to the initial formation.

(6) Patterns of a simple parameter, the Laplacian of the thermal advection for the layer 1000–700 mb., gave a good first approximation to the more elaborately derived

low-level convergence patterns (see par. 3 above), and were, in general, qualitatively consistent with precipitation patterns.

It is the considered opinion of the author that 300-mb. vorticity advection charts and Laplacian of thermal advection charts for the 1000-700-mb. layer (except over high terrain) would be useful guides in the forecasting of initial cyclone development at sea level and of associated precipitation patterns.

#### ACKNOWLEDGMENTS

The writer wishes to acknowledge his indebtedness to Prof. S. Petterssen, Miss D. L. Bradbury, and Drs. C. W. Newton and M. Estoque for their kind assistance in the preparation of this study.

#### APPENDIX—SYMBOLS AND EQUATIONS

The equations and symbols used are given below. For a more complete discussion, see Appendix I to Petterssen and Bradbury [3].

1. *Symbols and defining relationships.*—Pressure  $p$  is used as vertical coordinate. The vertical velocity  $\omega$  is expressed by

$$(1.1) \quad \omega = \frac{dp}{dt}$$

where  $t$  is time. The equation of continuity is written

$$(1.2) \quad D = -\frac{\partial \omega}{\partial p}$$

where  $D$  is horizontal divergence of the wind field represented on pressure contour charts.

The vertical component of the absolute vorticity is replaced by the geostrophic absolute vorticity  $Q$ , viz.,

$$(1.3) \quad Q = \frac{g}{f} \nabla^2 z + f$$

where  $z$  is the height of an isobaric surface,  $f$  is the Coriolis parameter, and  $\nabla^2$  is the Laplacian operator on an isobaric surface.

The advection of any quantity  $x$  is defined as:

$$A_x = -\mathbf{V} \cdot \nabla x$$

where  $\mathbf{V}$  is the velocity vector on an isobaric surface and  $\nabla$  is the gradient operator. Thus, the advection is positive or negative according as the wind is from high to low, or low to high, values of  $x$ .

If  $h$  is the thickness of an isobaric layer, the thickness advection is written:

$$(1.4) \quad A_h = -\bar{\mathbf{V}} \cdot \nabla h$$

Similarly, the vorticity advection at the level of non-divergence  $L$  is written:

$$(1.5) \quad A_{QL} = -(\mathbf{V} \cdot \nabla Q)_L$$

2. *Development.*—Following Sutcliffe [6] the amount of convergence  $-D$  is taken as a measure of development. Thus,

$$(2.1) \quad -D = \frac{1}{Q} \frac{dQ}{dt} = \frac{1}{Q} \left( \frac{\partial Q}{\partial t} + \mathbf{V} \cdot \nabla Q + \omega \frac{\partial Q}{\partial p} \right)$$

If  $\mathbf{C}$  is the velocity with which a motion system (e. g., a cyclone) moves, and  $\delta Q/\delta t$  is the local rate of change of  $Q$  at a point that retains its position relative to the moving system, we have:

$$(2.2) \quad \frac{\delta Q}{\delta t} = \frac{\partial Q}{\partial t} + \mathbf{C} \cdot \nabla Q$$

and

$$(2.3) \quad -D = \frac{1}{Q} \left( \frac{\delta Q}{\delta t} + (\mathbf{V} - \mathbf{C}) \cdot \nabla Q + \omega \frac{\partial Q}{\partial p} \right)$$

At sea level (or 1000 mb.)  $\omega = 0$

and

$$(2.4) \quad -D = \frac{1}{Q} \left( \frac{\delta Q}{\delta t} + (\mathbf{V} - \mathbf{C}) \cdot \nabla Q \right)$$

Thus, except at the vorticity center, this convergence contributes to intensification  $\delta Q/\delta t$  as well as motion.

With the symbols defined above, the development equation for sea level (see Petterssen [1]) is written:

$$(2.5) \quad -D_0 Q_0 = A_{QL} + \mathbf{V}_0 \cdot \nabla Q_0 - \frac{g}{f} \nabla^2 A_h - \frac{R}{f} \nabla^2 \left[ \log \frac{p_0}{p} \left( \overline{\omega(\Gamma_a - \Gamma)} + \frac{1}{c_p} \frac{dW}{dt} \right) \right]$$

Here, subscript naught refers to sea level (or 1000 mb.) and the bar denotes the mean value from 1000 mb. to this level of nondivergence,  $\Gamma_a = dT/dp$ ,  $\Gamma = \partial T/\partial p$ ,  $c_p$  is specific heat at constant pressure,  $dW/dt$  is the heat (other than latent) supplied to a unit mass per unit time,  $T$  is absolute temperature, and  $R$  is the gas constant.

Since

$$\frac{\partial Q_0}{\partial t} + \mathbf{V}_0 \cdot \nabla Q_0 = -D_0 Q_0$$

the foregoing equation may be written:

$$(2.6) \quad \frac{\partial Q_0}{\partial t} = A_{QL} - \frac{g}{f} \nabla^2 A_h - \frac{R}{f} \nabla^2 \left[ \log \frac{p_0}{p} \left( \overline{\omega(\Gamma_a - \Gamma)} + \frac{1}{c_p} \frac{dW}{dt} \right) \right]$$

Since the terms within the brackets cannot be evaluated routinely, an attempt was made to account for the observed vorticity tendency  $\frac{\partial Q_0}{\partial t}$  at sea level by using the simplified equation

$$(2.7) \quad \frac{\partial Q_0}{\partial t} = A_{QL} - \frac{g}{f} \nabla^2 A_h$$

3. *Vertical Velocity*.—This was computed only over the sea level center. From equations (2.2) and (2.3), one obtains:

$$(3.1) \quad \frac{\frac{\partial Q}{\partial t} + \mathbf{V} \cdot \nabla Q - \mathbf{C} \cdot \nabla Q}{Q^2} = \frac{\partial}{\partial p} \left( \frac{\omega}{Q} \right)$$

or

$$(3.2) \quad \int_{p_1}^{p_2} \frac{\frac{\partial Q}{\partial t} + \mathbf{V} \cdot \nabla Q - \mathbf{C} \cdot \nabla Q}{Q^2} dp = \left( \frac{\omega}{Q} \right)_0 - \left( \frac{\omega}{Q} \right)_1$$

Using the boundary condition that  $\omega_0$  vanishes at sea level ( $p_0 = 1000$  mb.) the vertical velocity was obtained for any higher level by columnar interpolation.

For a discussion of accuracy of such computations and the difficulties encountered, reference is made to Petterssen and Bradbury [3].

#### REFERENCES

1. S. Petterssen, "A General Survey of Factors Influencing Development at Sea Level," *Journal of Meteorology*, vol. 12, No. 1, Feb. 1955, pp. 36-42. (See also *Technical Report No. 3*, Dept. of Meteorology, University of Chicago, 1954.)
2. S. Petterssen, G. E. Dunn, and L. L. Means, "Report of an Experiment in Forecasting of Cyclone Development," *Journal of Meteorology*, vol. 12, No. 1, Feb. 1955, pp. 58-67. (See also *Technical Report No. 4*, Dept. of Meteorology, University of Chicago, 1954.)
3. S. Petterssen and D. L. Bradbury, "An Investigation of Cyclone Development, Storm No. 1," *Technical Report No. 5*, Dept. of Meteorology, University of Chicago, 1954.
4. S. Petterssen, "On the Propagation and Growth of Jet-Stream Waves," *Quarterly Journal of the Royal Meteorological Society*, London, vol. 78, No. 337, July 1952, pp. 337-353.
5. J. F. Appleby, "Trajectory Method of Making Short-Range Forecasts of Differential Temperature Advection, Instability, and Moisture," *Monthly Weather Review*, vol. 82, No. 11, Nov. 1954, pp. 320-334.
6. R. C. Sutcliffe, "A Contribution to the Problem of Development," *Quarterly Journal of the Royal Meteorological Society*, London, vol. 73, No. 317-318, July/Oct. 1947, pp. 370-383.

## Water Supply Forecasts for the Western United States

Published monthly from January to May, inclusive. Contains text, map, and tabulations of water-year and seasonal runoff forecasts for the eleven Western States, by Weather Bureau, Soil Conservation Service, and the State of California. For copies of the 1956 forecasts apply to River Forecast Center, Weather Bureau Office, 712 Federal Office Building, Kansas City 6, Mo.

# SOME METEOROLOGICAL ASPECTS OF DROUGHT

## WITH SPECIAL REFERENCE TO THE SUMMERS OF 1952-54 OVER THE UNITED STATES

JEROME NAMIAS

Extended Forecast Section, U. S. Weather Bureau, Washington, D. C.

[Manuscript Received August 4, 1955]

### ABSTRACT

The problem of drought is examined as a manifestation of anomalous patterns of the atmosphere's general circulation. Special consideration is given to the quasi-stationary planetary wave ensembles which are responsible for extensive summertime drought over the United States. The critical importance of the great Atlantic and Pacific anticyclones for encouraging or discouraging the development of the great North American upper level anticyclone, the immediate drought producing cell, is emphasized.

### 1. INTRODUCTION

The term drought has never been given a quantitative definition acceptable to everyone. In loose terms it is an extended period characterized by lack of precipitation, the consequence of which is generally reflected in some important phase of the changing economy. Under this definition dry spells in areas at times when little or no rain normally falls are not considered drought periods, and the *anomalous* character of precipitation is an important part of the definition. It is this phase of the subject which shall be discussed in this article with particular emphasis on the departures of precipitation from long-term normals (the climatic anomalies of precipitation) as they relate to the atmosphere's broad-scale or general circulation.

Although forever attempting to approach some sort of equilibrium the atmosphere's circulation is never at rest. On a grand scale it has various modes of operation so that during a particular month the air currents composing the circulation may assert themselves in a similar manner on many days of the month. In this way the patterns of air flow have *prevailing* characteristics and these may be brought to light by averaging weather maps over the entire month. Such a chart for the month of October 1952 is shown in figure 1, where the averaging process has by no means damped out the planetary waves.

### 2. CONDITIONS LEADING TO DROUGHT DURING MONTHS OTHER THAN SUMMER

If the arrangement of planetary waves of the general circulation were to remain stationary those areas ahead of the troughs would receive bountiful precipitation while those behind the troughs and in the ridges would, because

of the lack of precipitation-producing cyclones, be dominated by dry conditions leading perhaps to drought. This relationship between precipitation and planetary wave, well known and demonstrable statistically [1], results from the prevailing upward motion of the air in advance of the midtropospheric troughs and the sinking motion behind. It is also associated with the development and movement of polar front waves ahead of the upper level trough.

While the planetary waves are never exactly stationary from day to day there are cases in which the broad-scale pattern remains quite similar for several days at a stretch and at times for as long as a fortnight or more. Such a case is illustrated by the conditions observed during October 1952 (fig. 1) which on a countrywide basis was the driest month ever observed in the history of the U. S. Weather Bureau [2]. From the resultant pattern of upper air flow for the month, in which the resultant winds blow parallel to the average contours shown in figure 1, it is apparent that most of the United States lay under the domination of either a strong ridge or a prevailing flow of air from the northwest. The troughs in which the storms were spawned and then steered northeastward were well off the Pacific Coast and along the Atlantic Coast. This particular pattern effectively shunts precipitation-producing storms away from the entire United States and also provides an efficient mechanism for inhibiting the influx of moist rain-bearing air masses from the Gulf of Mexico. Note that only Florida was materially affected by these air masses.

In a similar manner extensive dry (or wet) periods may be created over large areas, providing the basic pattern of upper level flow has a more or less characteristic geographical preference. It turns out that the day-to-day stability of the planetary wave pattern during October 1952 was much greater than is usually observed, or in

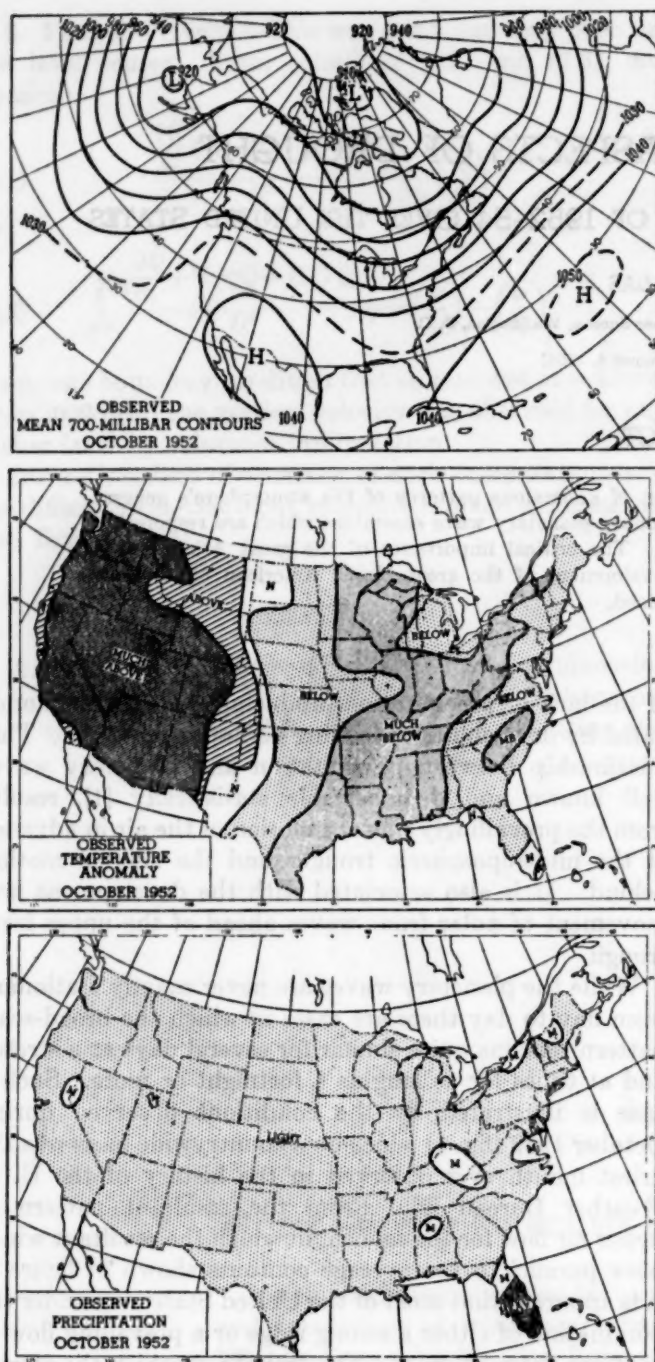


FIGURE 1.—(Top) Average 700-mb. height contours (labeled in tens of feet), October 1952. The average or resultant air flow blows parallel to the contours with lower heights to the left of the flow. (Middle) Classes of temperature departures from normal for October 1952. (Bottom) Classes of precipitation observed in October 1952, the driest month ever recorded in the United States. (Light, moderate, and heavy refer to terciles computed from many years of past Octobers.)

other words, the planetary wave patterns possessed remarkable persistence from day to day and even from week to week. The more common case is for the basic pattern to break down (or change) completely for a brief period (perhaps a few days or a week) only to reemerge

and persist later on. The latter phenomenon is not so much a persistence of pattern as a persistent recurrence which thereby provides a bias in monthly (or longer period) averages of both flow pattern and associated meteorological elements.

Thus the central problem of drought revolves around the fact that it is a manifestation of certain recurrent forms of the general circulation, and therefore its prediction demands a fuller understanding of the mechanics of the general circulation.

### 3. SUMMERTIME DROUGHT

Precipitation deficiencies over intracontinental areas of temperate latitudes during summer are apt to have serious consequences on the economy. This is because a good proportion of the normal annual rainfall occurs in these areas at this time of year and because high temperatures then, usually associated with lack of rain, cause desiccation. The resulting effects on crops, livestock, and water supply in general are well recognized.

The atmospheric general circulation during summer drought has a quite characteristic pattern, and here again this pattern is brought into sharpest focus at levels well removed from the surface. In the normal course of transition from winter to summer the prevailing westerlies of temperate latitudes migrate northward. The jet stream with its planetary waves also engages in this migration. The magnitude of the shift is of the order of  $10^\circ$  of latitude from about  $30^\circ$  N. latitude in winter to  $40^\circ$  N. latitude in summer. South of the crests of the planetary waves the belt of light wind flow and higher pressure fractures into great cells around which the air rotates in a clockwise manner. These cells are frequently the upper level components of the subtropical Highs at the surface, although over continents the surface anticyclone may be absent.

The air comprising these upper level cells comes largely from the prevailing westerlies to the north and slowly subsides to lower elevations [3]. In sinking, the air masses are warmed by compression, and consequently, the areas underlying these cells are characterized by abnormal warmth and by lack of clouds and rainfall.

The drought of 1936 may serve as an example. In figure 2 is shown the average pattern of flow at the 700-mb. level for August of that year and the associated departures from normal of temperature, while the corresponding departures of rainfall are shown in the inset of figure 3. In figure 2 it may be noted that over lower latitudes there is a great girdle of high pressure which consists of several cells. One of these overlies southern United States and is associated with temperatures averaging as high as  $10^\circ$  above seasonal normals in Missouri and Kansas, along with deficits of rainfall of from 2 to 4 inches over a broad area. Figure 3 shows the moisture characteristics of the prevailing air currents affecting the drought area during this month. This chart is not constructed for a constant level, but rather for an isentropic surface, along which air parcels are more or less constrained to move. Dry currents emanat-

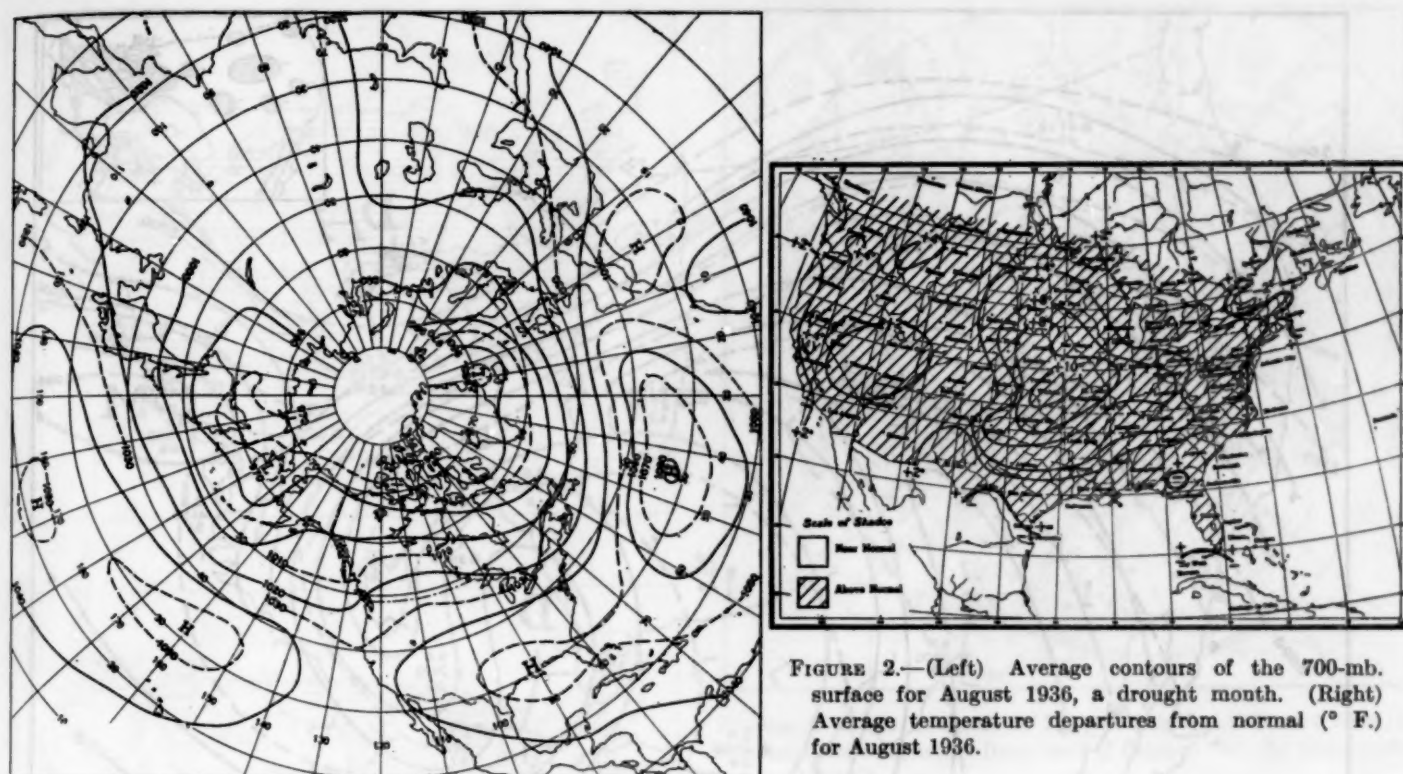


FIGURE 2.—(Left) Average contours of the 700-mb. surface for August 1936, a drought month. (Right) Average temperature departures from normal ( $^{\circ}$  F.) for August 1936.

ing from high levels over Canada crossed the Great Lakes, flowed along and off the Atlantic Seaboard into Florida, and then spiraled into the anticyclonic cell over the Gulf States, subsiding gradually in transit [3]. Moist tongues of air arriving from the western Gulf of Mexico and the western Plateau were rapidly depleted of their moisture by being cut off and mixed with the flanking drier air currents.

Explanations of summertime drought hinge in large part on the position, extent, and development of these upper level semipermanent anticyclonic cells. This will be made clearer by discussion of the recent period of drought during the summers of 1952 through 1954.

#### 4. SUMMER DROUGHT OF 1952-54

During the summers of 1952-54 the prevailing patterns of large-scale air flow and the resulting patterns of temperature and precipitation over the United States were quite similar. Therefore average charts constructed for the three summers, based on Junes, Julys, and Augusts of these years, effectively bring out the dominant characteristics of the triennium. The temperature and precipitation departures for the country shown in figure 4 illustrate the prevailing hot and dry nature of south central portions.

The average pattern of air flow at the 700-mb. level for the three summers is shown in figure 5 by light solid lines. From these it is apparent that a great anticyclonic cell once more dominated south central United States and that other similar cells were located over the adjacent oceans.

Since drought is an abnormal phenomenon we are interested not only in the broad-scale patterns of air flow with which it is associated, but also in the *anomalous* character of this flow. One effective means of portraying this is by subtracting from the drought-producing pattern the normal pattern, as has been done in figure 5. The heavy broken lines thus represent departures from normal of the height of the 700-mb. surface during the three summers of 1952-54. As with the contours, the prevailing *anomalous* component of the upper air flow may be deduced by noting that it flows parallel to the heavy broken lines in the sense that higher values always lie to the right of the anomalous flow. Thus the prevalence of much more than normal easterly and northeasterly flow along the Gulf Coast, inhibiting the northward penetration of deep moisture-laden air masses from the Gulf of Mexico, is clearly shown.

The anomalous areas shown by the broken lines also illustrate other interesting features. For example, two large positive anomalies also suggestive of dryness appear over the central Pacific and central Atlantic. On the other hand the negative centers over Western Europe and northwestern United States were associated with prevailingly wet and cool weather.

The positive anomalies over the oceans are of a special importance because they deserve a good deal of the blame for the drought associated directly with the anomalous cell over the United States. The reason for this is that component parts of the planetary wave system, including the subtropical high pressure cells to the south of the wave crests, are not independent of one another but are interdependent [4]. That is, each cell has an influence on each

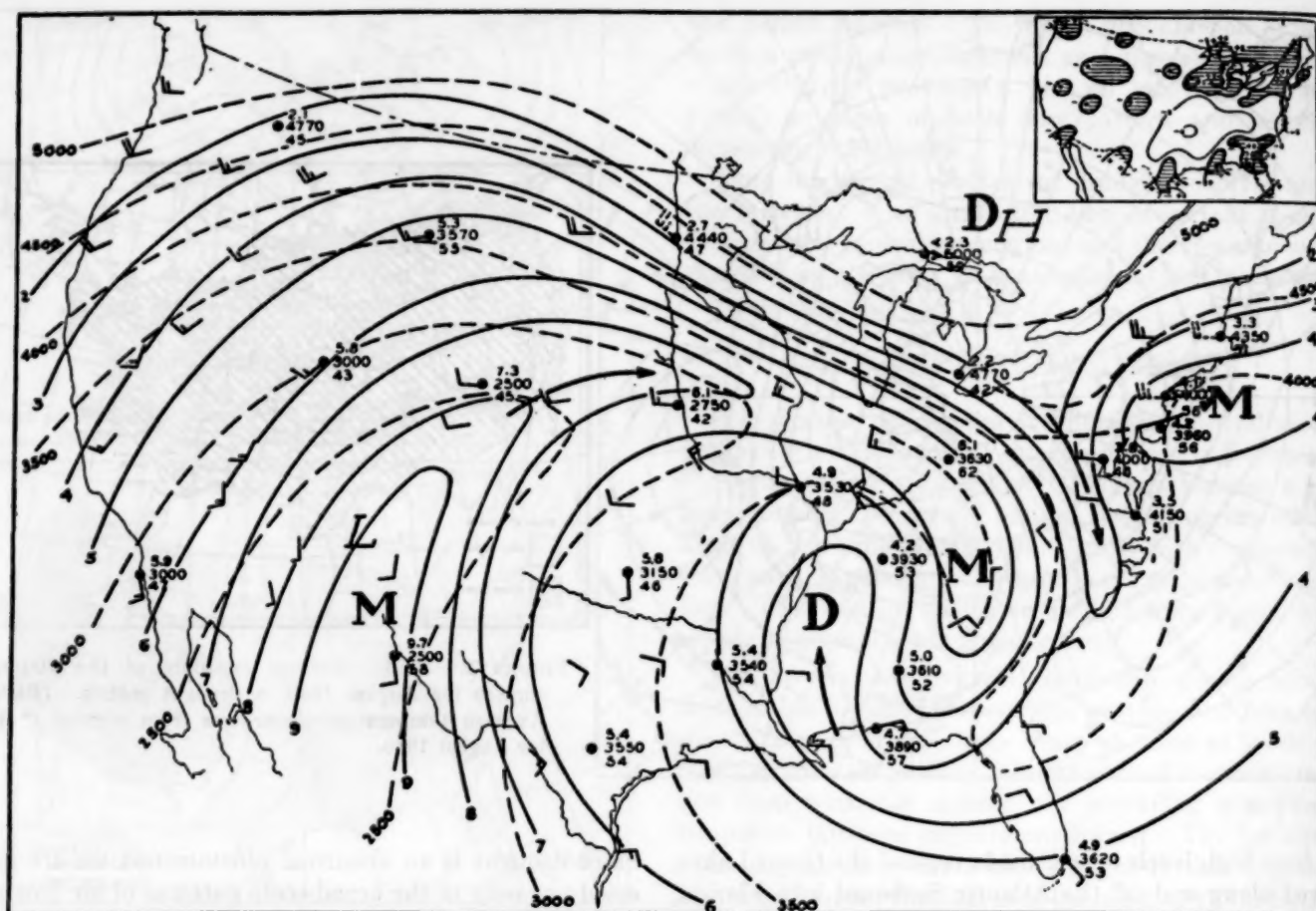


FIGURE 3.—Mean isentropic chart for the potential temperature surface 315° A. for August 1936. Height contours (broken lines) are labeled in meters above sea level. The average moisture content of the air at this surface (in g/kg) is shown by solid lines. Moist and dry tongues are labeled M and D. Inset shows the departure from normal of precipitation in inches.

other cell of the hemisphere. Stable wave lengths of the planetary waves depend upon complex dynamical and thermodynamical effects induced largely by underlying terrain. If for some reason a certain disturbance in the westerlies is constantly being generated in one area, the absolute vorticity of air columns leaving this area will set up certain resonant features of flow in other, even remote, areas. In this manner disturbances formed in various areas may be reinforcing or conflicting, both in the regions at the seat of the disturbances and also in areas between. Since the present state of meteorological theory is inadequate to tell very much about these influences over time intervals of more than a day or two, empirical work has been necessary to substitute for physical understanding.

One of these empirical approaches [5] has been to select from past years those average maps (in this case 700-mb. maps for 5-day periods) characterized in a certain season by a large positive or negative anomaly in a given area. One may then determine the probability of sign of anomaly, positive or negative, in other areas of the hemisphere, adjacent to and remote from the selected area. When this has been done a chart like figure 6 results. The selected area

of positive anomaly in this figure is hatched and lines of equal probability of sign are drawn for each 10 percent. For example, figure 6 indicates that when a positive anomaly center appears in the hatched area in summer there is a probability of over 80 percent that the accompanying anomaly will be negative over much of the State of Washington and over 70 percent that it will be positive over New England. It may be demonstrated statistically that higher probabilities usually go with higher mean values of the anomaly itself, so that, in a general sense, isolines of probability may be interpreted similarly to isolines of anomaly.

From figure 6 it is clear that the Pacific cell of positive anomaly has a resonance effect over the United States which accounts for some of the features observed in the 1952-54 pattern. But the Pacific cell is only one of the influences which may affect the United States cell. Since the Atlantic cell is equally prominent in figure 5, having a +10 anomaly, another probability chart similar to figure 6 but selected for the location of the Atlantic cell was used (not reproduced). A mean of the two probability charts based on Atlantic and Pacific fixes was prepared in order to capture the resonance effects of both Atlantic

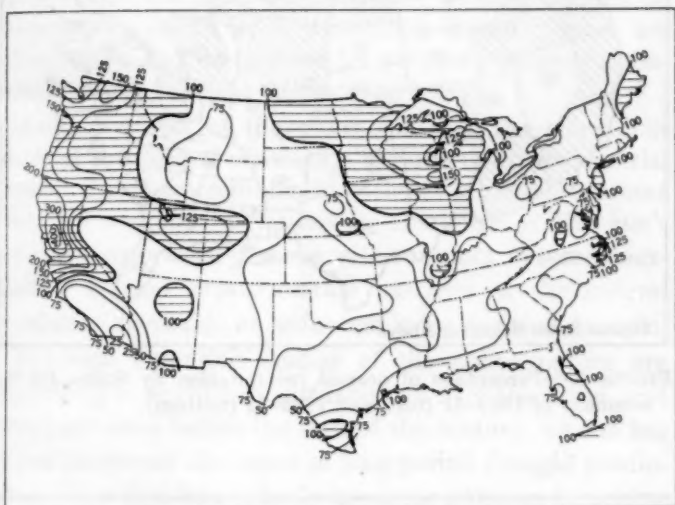
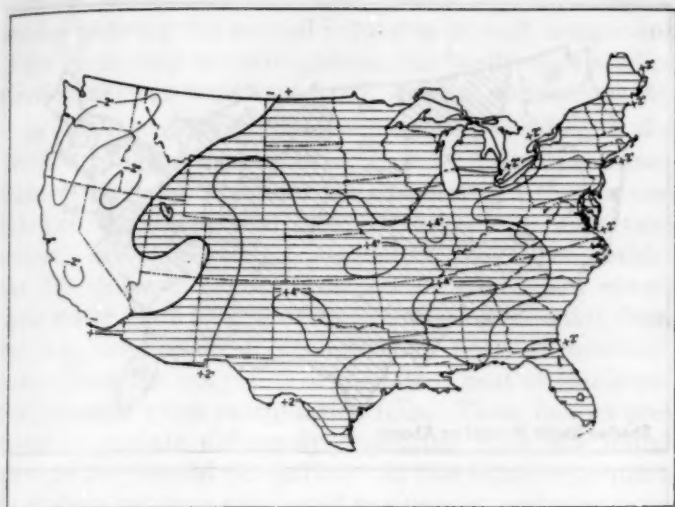


FIGURE 4.—(Top) Average temperature departures from normal ( $^{\circ}$  F.) for the three drought summers (June, July, and August) of 1952-54. (Bottom) Percentage of normal precipitation for the summers 1952-54.

and Pacific on the North American pattern, and this combined chart is shown in figure 7. It is obviously not surprising to find similarity in pattern over the oceans in figures 7 and 5, for these areas constituted the basis of selection. On the other hand the similarity of pattern over North America is indeed striking, since the data there are entirely independent. This correspondence indicates that the great drought-producing cell for the summers of 1952-54 needed for its sustenance companion cells in both Atlantic and Pacific.

##### 5. CONTRAST WITH PRECEDING 3 YEARS, 1949-51

During 1949-51 the summertime weather and circulation regimes over the United States were quite different from those during the subsequent three summers. The contrasting precipitation regimes are shown in figure 8, where the areas affected by drought in the later 3 years, were actually abnormally wet in the summers of 1949-51.

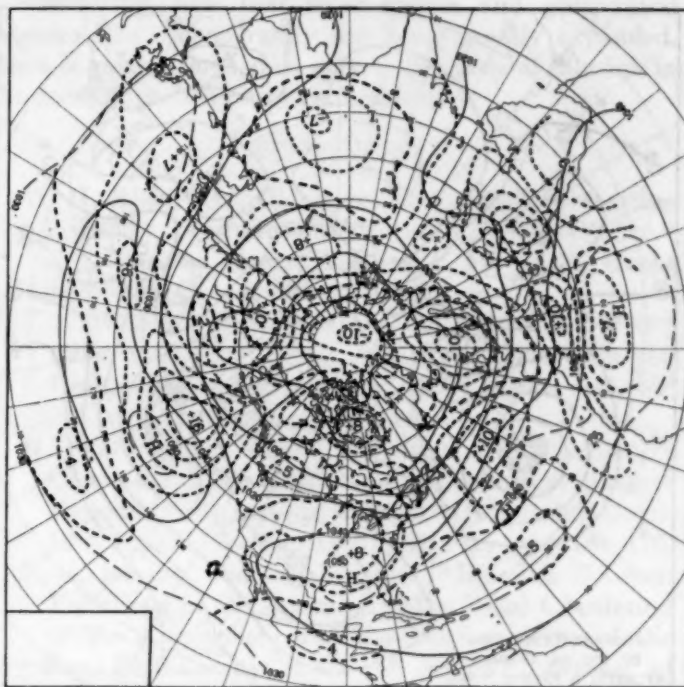


FIGURE 5.—Mean contours of 700-mb. height (solid) and lines of equal height departure from normal (broken) for the three summers 1952-54.

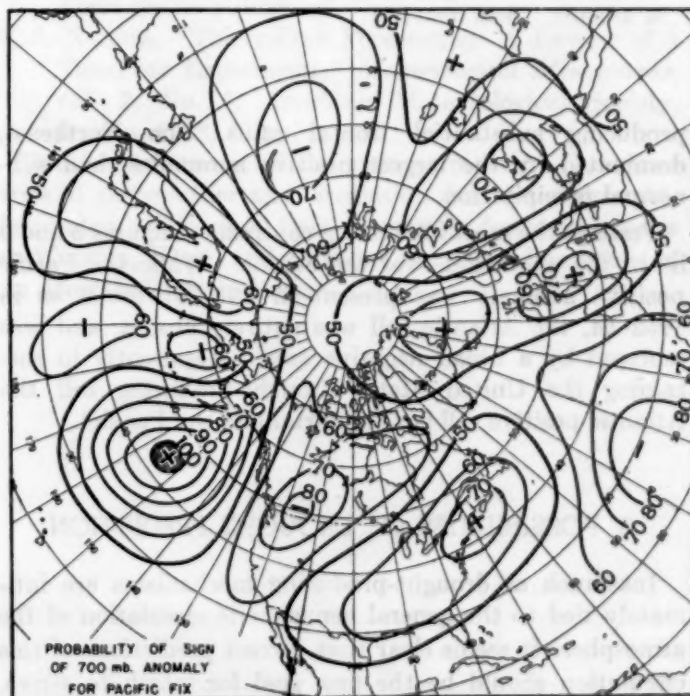


FIGURE 6.—Probability of sign of 700-mb. height anomaly when an axis of positive anomaly lies in the vicinity of the hatched area in the Pacific in summer. (From [5].)

The patterns of circulation (fig. 9) were also materially different. In 1949-51 no strong anticyclonic cell or positive anomaly was present over the Gulf States. Anomalous northerly flow from Canada entered the Great Plains to converge with southerly transported Gulf air,

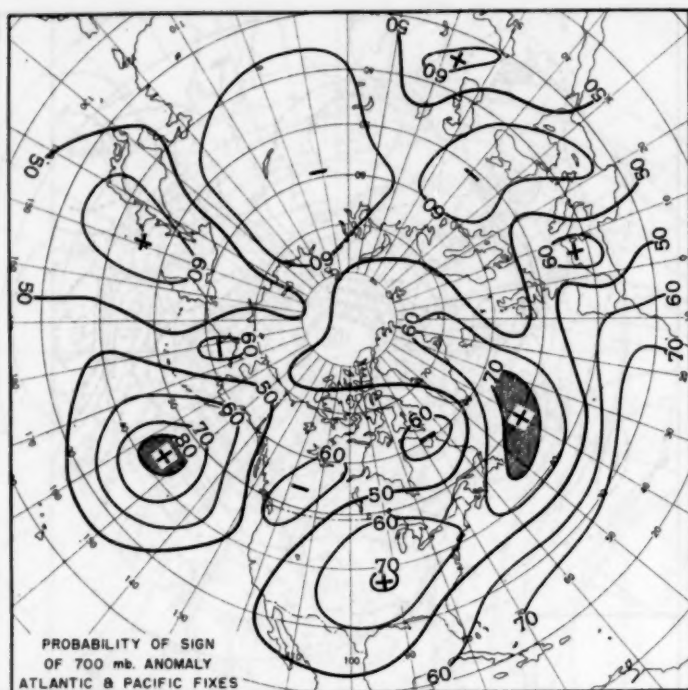


FIGURE 7.—Probability of sign of 700-mb. height anomaly when axes of positive anomaly lie in the vicinity of the hatched areas shown in the Pacific and Atlantic in summer. (This is a mean of chart shown in fig. 6 and chart selected for positive anomaly in Atlantic. Both from [5].)

producing substantial frontal rains. The Northeast, dominated by the largest positive anomalies, had sub-normal precipitation.

Perhaps the most interesting contrasts of figures 5 and 9 lie in the anomalies over the oceans. While the Pacific positive anomaly was present in 1949–51 much as in 1952–54, the Atlantic cell was entirely absent, and was replaced by a broad negative area. Apparently in sustaining the United States drought-producing cell the Atlantic positive cell is as important as the Pacific!

## 6. POSSIBILITIES OF DROUGHT PREDICTION

Inasmuch as drought-producing mechanisms are intimately tied to the general hemispheric circulation of the atmosphere it seems clear that correct predictions of this circulation should be the first goal for which to strive. Methods which show a moderate degree of success have been developed for 5- and 30-day periods. The latter predictions for example, were quite successful in catching the initiation of the 1953 and 1954 summer drought patterns as well as the October 1952 pattern shown in figure 1.

These 5- and 30-day forecasts are based largely upon long-period trends observed in series of average charts for upper atmospheric levels, upon the expected influences of

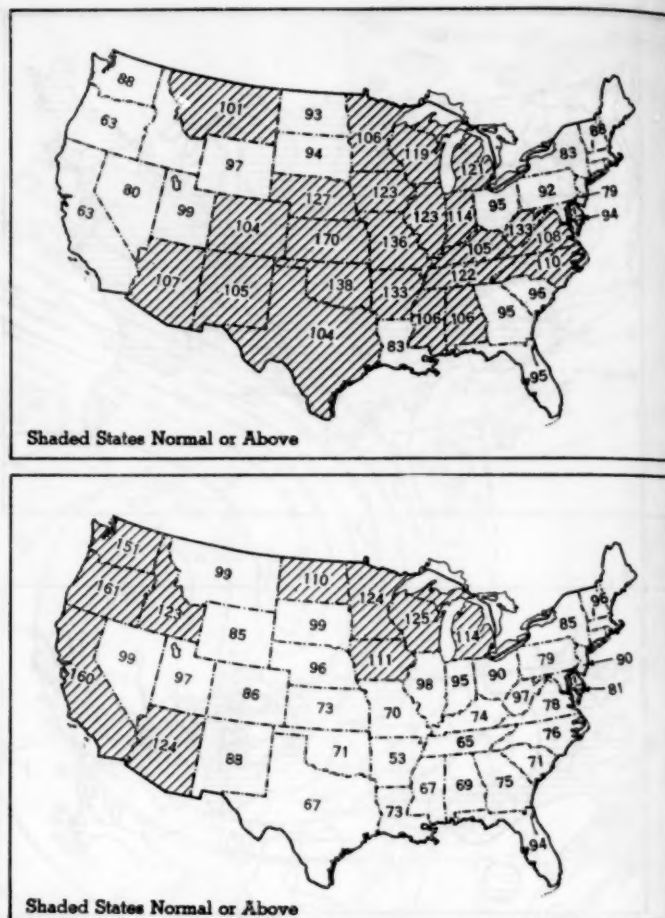
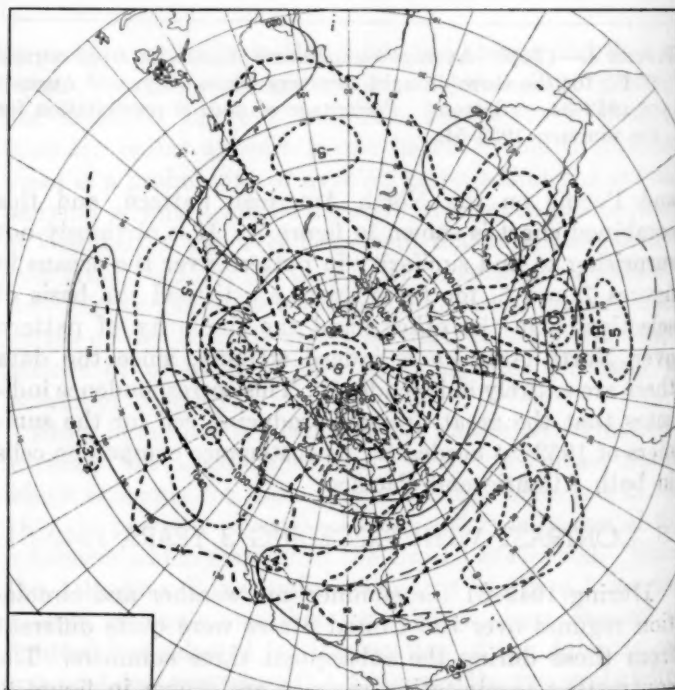


FIGURE 8.—Percentage of normal precipitation by States for the summers of 1949–51 (top) and 1952–54 (bottom).



seasonal transitions on these trends, upon empirical studies showing the mutual influences of each component of the circulation on its neighbors, and finally upon studies relating average weather to such average circulations [6].

In this methodology no direct account is taken of the detailed physical aspects of how or why such persistent features are established, for the simple reason that no one yet knows much about these fundamentally important topics. To name only a few pertinent factors, one might cite the differing effect of various surfaces (snow cover, open water, bare land, etc.) upon incoming radiation from the sun, the impact upon various air flows of mountain chains, and the net result of the latent heat of condensation released when precipitation falls. These factors presumably operate differently depending upon the initial state of the general circulation. In this sense subsequent anomalous patterns are viewed as a natural evolution from preceding patterns which are themselves anomalous. In other words, the circulation changes, whether treated on the scale of a day, a week, a month, a season or more, are self-evolving and are guided by an ever-changing radiational balance incident to changing season.

Another school of thought holds that the anomalous states of the general circulation are due to extraterrestrial causes. The more common hypotheses of this sort assume that the irregular variations in character of the sun's radiation, associated perhaps with sunspots, in some unexplained manner create certain patterns of the general circulation favorable or unfavorable for regional drought.

Although extensive studies of the above nature are proceeding in scientific institutions all over the world, and have been since before the turn of the century, no one has as yet uncovered the secret of long-period drought prediction. Now that hemispheric upper-air data are becoming reasonably extensive and a backlog of many years is

accumulating, now that solar science and geophysical sciences like oceanography are being greatly expanded, there is greater hope than ever that a general solution to the drought problem may be forthcoming.

#### REFERENCES

1. W. H. Klein, "An Objective Method of Forecasting Five-Day Precipitation for the Tennessee Valley," U. S. Weather Bureau *Research Paper* No. 29, Washington, D. C., April 1949, 60 pp.
2. J. S. Winston, "The Weather and Circulation of October 1952—the Driest Month on Record in the United States," *Monthly Weather Review*, vol. 80, No. 10, Oct. 1952, pp. 190–194.
3. H. Wexler and J. Namias, "Mean Monthly Isentropic Charts and Their Relation to Departures of Summer Rainfall," *Transactions, American Geophysical Union* 19th Annual Meeting, April 1938, Part 1, pp. 164–170.
4. C.-G. Rossby, and collaborators, "Relation Between Variations in the Intensity of the Zonal Circulation of the Atmosphere and the Displacements of the Semi-Permanent Centers of Action," *Journal of Marine Research*, vol. 2, No. 1, Jan. 1939, pp. 38–55.
5. D. E. Martin, Anomalies in the Northern Hemisphere 700-mb. 5-day Mean Circulation Patterns, 1953, AWSTR 105–100, Air Weather Service, U. S. Air Force (to be published).
6. J. Namias, "Thirty-Day Forecasting: A Review of a Ten-Year Experiment," *Meteorological Monographs*, vol. 2, No. 6, American Meteorological Society, Boston, 1953, 83 pp.

Detailed treatment of the average monthly characteristics of the weather and circulation during the drought-dominated summers of 1952–54 may be found in articles by Winston, Klein, and Hawkins in appropriate issues of the *Monthly Weather Review*.

# THE WEATHER AND CIRCULATION OF SEPTEMBER 1955<sup>1</sup>

ARTHUR F. KRUEGER

Extended Forecast Section, U. S. Weather Bureau, Washington, D. C.

## 1. WEATHER AND CIRCULATION OVER THE UNITED STATES

During September 1955 surface temperature anomalies over the United States underwent a complete reversal

(fig. 1). Early in the month (fig. 1a) temperatures averaged above normal in the North and West and below normal in southern and central portions. Within this

<sup>1</sup> See Charts I-XV following p. 215 for analyzed climatological data for the month.

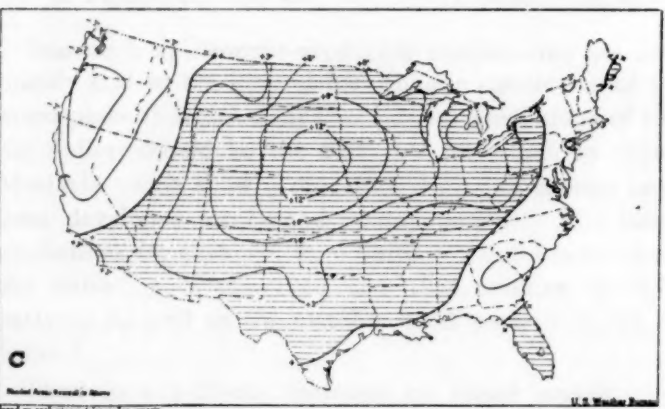
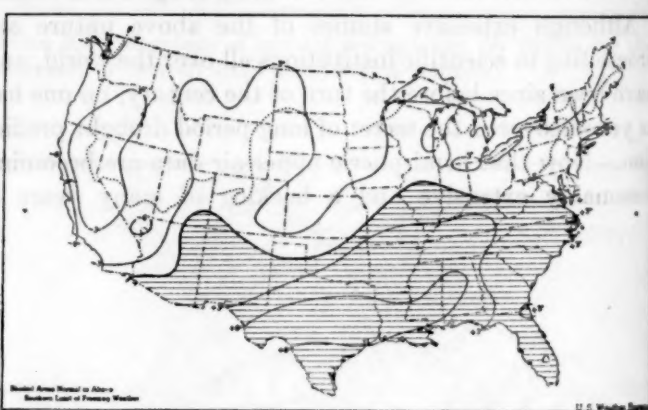
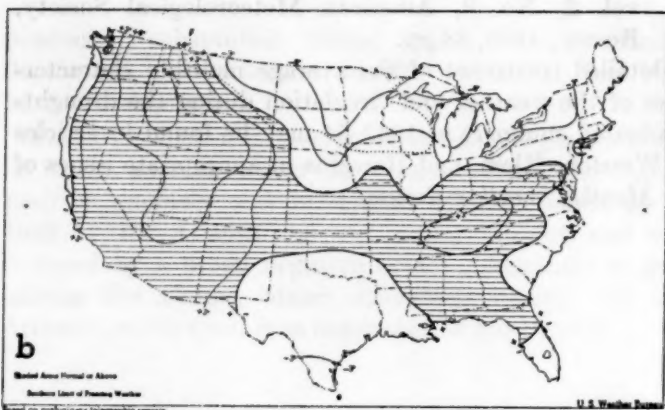
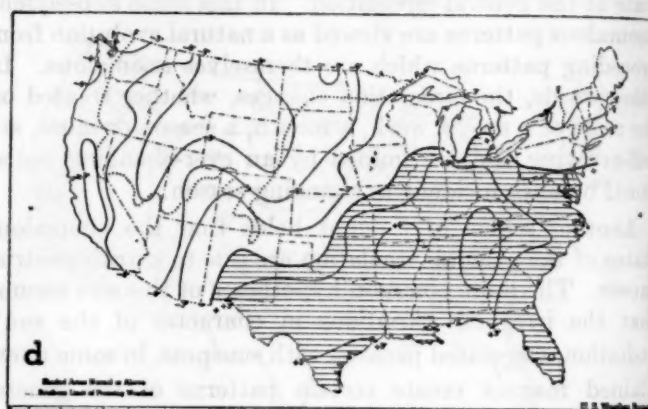
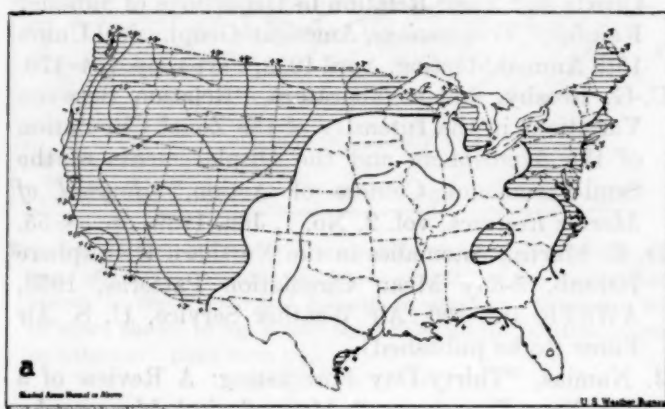


FIGURE 1.—Departure of average temperature ( $^{\circ}$ F.) from normal for weeks ending (a) September 4, (b) September 11, (c) September 18, (d) September 25, and (e) October 2, 1955. Cold replaced heat as the trough established itself in the West.

period the West experienced a particularly intense heat wave with temperature readings ranging as high as 110° F. at Los Angeles, 111° F. at Red Bluff, Calif., and 107° F. at Medford, Oreg. At Los Angeles, beginning with August 31, over 100° readings continued for 8 successive days, setting a record for September heat. This heat moderated by the middle of the month (fig. 1c) and temperatures even became subnormal, while 100° readings now appeared briefly in the central part of the country as far north as Pierre, S. Dak. Later this month a warming trend occurred in the Southeast, accompanied by marked cooling in the North and West (fig. 1d and e). It was within this period that Jackson, Miss., after 3 months of below normal temperatures, experienced its highest temperature of the year, 97° F., on September 20.

These temperature changes accompanied a readjustment in the long wave pattern over North America, as is seen from figure 2A and B. The first half of the month was characterized by a ridge and above normal 700-mb. heights in the West and a weak trough in the East. As pointed out frequently in past articles of this series, such conditions usually accompany above normal temperatures in the West. The easterly anomalous flow in the Southwest further contributed to heating due to compression of the air as it descended the mountains into California, resulting in the abnormally high temperatures referred to above.

The latter half-month witnessed the establishment of a diametrically opposite pattern across the continent (fig. 2B). The ridge in the West gave way to a trough, with heights as far below normal as they had been above earlier in the month. The weak trough in the East similarly was replaced by a ridge. As this pattern came into being below normal temperatures occurred in the West and above normal in the Southeast (fig. 1d).

This circulation change accompanied a southward shift of the westerlies from their abnormal northerly position during August [1] to temperate latitudes in September. This is shown in figure 3, where it is seen that from August to September the westerlies diminished north of 55° N. and increased markedly in midlatitudes. This change occurred near the middle of the month as the zonal westerlies (35°N.-55°N.) reached their maximum value of the month and the polar westerlies were diminishing most rapidly. This southward shift of the strongest westerlies weakened the subtropical ridge in the United States (except for the Southeast) by allowing cooler air masses to penetrate the country (Chart IX).

The distribution of precipitation during the month similarly reflected this change in circulation. The first half of the month produced negligible precipitation amounts, except along the Gulf and South Atlantic coasts. This was a consequence of northerly and northwesterly flow over much of the country, a circulation pattern which has been recognized as characteristic of dry weather over most of the United States during September [2] as well as in the winter season [3, 4]. With the trough development

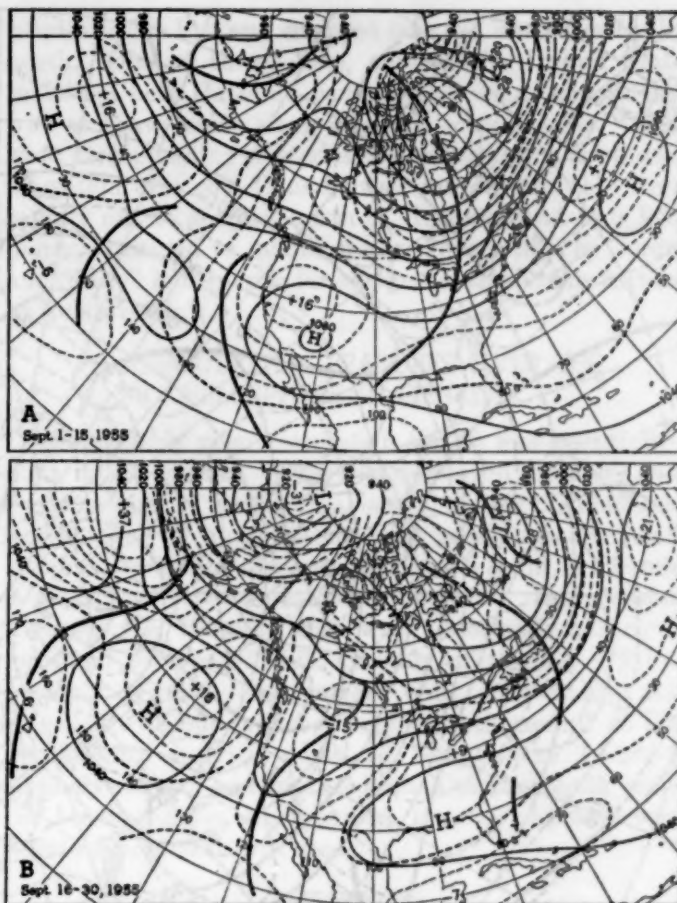


FIGURE 2.—Mean 700-mb. contours for 15-day periods (A) September 1-15, and (B) September 16-30, 1955 with departure from normal superimposed (both in tens of feet). Above normal heights in the West gave way to below normal heights.

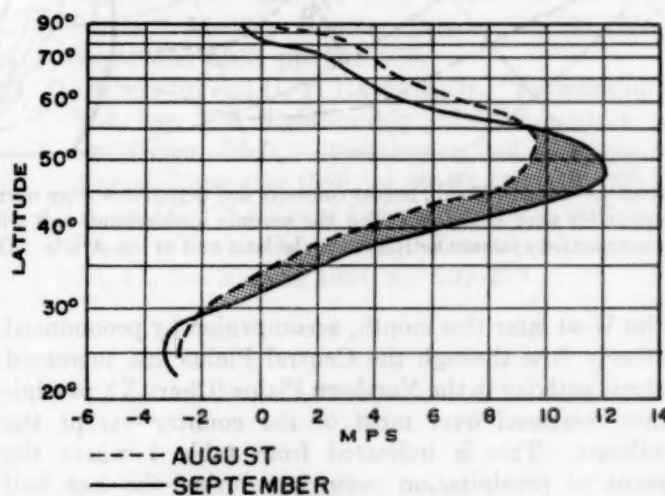


FIGURE 3.—Mean zonal wind speed profile (0° westward to 180°) for September 1955 (solid) and August 1955 (dashed). Latitudes where the zonal wind speed increased over the August values are shaded. Marked increases occurred south of 55° N. latitude with decreases north of this latitude.

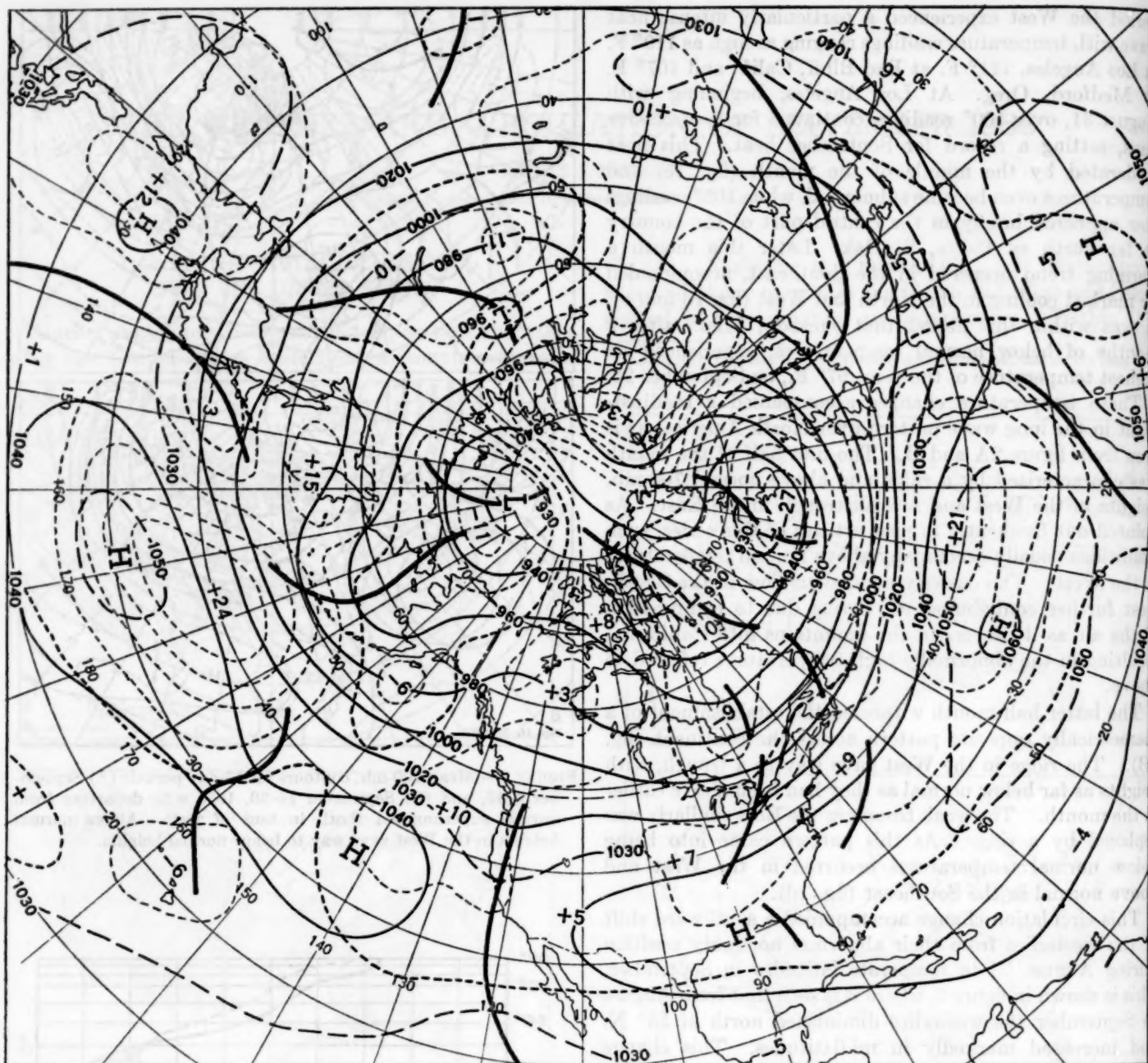


FIGURE 4.—Mean 700-mb. height contours and departures from normal (both in tens of feet) for September 1955. Largest positive height anomalies were associated with the oceanic anticyclones and with blocking north of Scandinavia, while greatest negative anomalies accompanied cyclonic activity near Iceland and in the Arctic. Over North America heights averaged slightly above normal.

in the West later this month, accompanied by pronounced southerly flow through the Central Plains and increased cyclonic activity in the Northern Plains (Chart X), precipitation increased over most of the country except the Southeast. This is indicated from table 1 where the percent of precipitation occurring during the last half of the month is tabulated for a few stations. Many stations in the Plains States received all of their monthly precipitation during the last 15 days. Even in the eastern part of the country, which early in the month lay under

cyclonically curved flow aloft, some stations still received as much as 90 percent of their rainfall the last half-month when the flow was anticyclonically curved. The explanation for this lies in the fact that early in the month most of the country, except the southeastern coastal areas, was under the influence of essentially continental and modified Pacific air masses, while later in the month moister air from low latitudes was carried northward and eastward as the trough in the West became established. In the southeastern part of the country some drying out occurred

TABLE 1.—Percentage of monthly precipitation occurring during last half of September 1955 at selected stations in the United States. Note that the southeastern stations in the right half of table received most of their rainfall in the first half of the month.

	Percent		Percent
Billings, Mont.	99	Charleston, S. C.	3
Kansas City, Mo.	100	Raleigh, N. C.	34
Amarillo, Tex.	100	Miami, Fla.	26
Huntington, W. Va.	90	Corpus Christi, Tex.	17
Syracuse, N. Y.	87	New Orleans, La.	17

the latter half-month as anticyclonic conditions set in. Some cities in this region received less than 30 percent of their monthly total during this period (table 1).

The circulation that resulted from averaging of these two regimes is seen in figure 4. Over the United States heights averaged slightly above normal with weak troughs present along the west coast and in the Great Lakes region. Temperatures associated with this mean circulation averaged essentially above normal with a few stations reporting positive departures of as much as 4°F. (Chart I-B). Precipitation amounts were heavier than normal along the Gulf and Carolina coastal areas, which received large amounts from tropical storms, and also in some central sections where local amounts as great as 6 inches occurred (Charts II and III). Subnormal amounts, on the other hand, occurred in the Northern Plains, the Southwest, and within the interior regions of some of the Gulf States under the subtropical ridge. Drought conditions in the Southeast under this subtropical high cell were particularly striking—Birmingham, Ala., for example, with only a trace of rain, experienced its driest September on record and its driest month since October 1924 when no rain occurred at all.

## 2. HURRICANE ACTIVITY

Six tropical storms, four of hurricane intensity, made their appearance this month in the waters adjacent to the North American coast (Chart X). Of these, three penetrated the Mexican coast, accompanied by torrential rains, high winds, and flooding, and caused considerable loss of life and property damage. These storms traversed the Caribbean parallel to the prevailing easterly flow aloft where 700-mb. heights averaged below normal. This track lay in the region of cyclonic shear to the left of the strongest easterlies, which were stronger than those for August south of 30° N. latitude (fig. 3).

Two hurricanes successfully penetrated the mean sub-

tropical ridge line and emerged into the westerlies farther north. One of these, Ione, entered the United States mainland near Hatteras, causing high winds and tides as well as heavy rains along adjacent coastal areas. However, strengthening westerlies accompanying a southward migration of a cool Canadian air mass swept this storm rapidly out to sea just north of Hatteras, and thus little damage resulted to inland areas. (See article by Jordan and Stowell in this issue for analysis of small-scale features of Ione's track.)

## 3. CIRCULATION FEATURES OVER THE HEMISPHERE IN GENERAL

The monthly mean circulation (fig. 4) was essentially a high index pattern with well-developed oceanic anticyclones north of their normal latitudes. At high latitudes well-marked cyclonic centers were present in the Arctic and in the vicinity of Greenland and Iceland, while mid-latitude troughs were weaker than normal. In the eastern Atlantic the 700-mb. flow was abnormally strong as indicated by the -270-ft. anomaly north of a +210-ft. anomaly center. This current split at the European coastline with one branch swinging north around an area of blocking activity north of Scandinavia (+340-ft. anomaly center), and another branch passing south across the Mediterranean accompanied, however, by only weak negative heights in this area.

## REFERENCES

1. J. Namias and C. R. Dunn, "The Weather and Circulation of August 1955—Including the Climatological Background for Hurricanes Connie and Diane," *Monthly Weather Review*, vol. 83, No. 8, August 1955, pp. 163-170.
2. W. H. Klein, "The Weather and Circulation of September 1953—Another Dry Month in the United States," *Monthly Weather Review*, vol. 81, No. 9, September 1953, pp. 304-308.
3. D. E. Martin and H. F. Hawkins, Jr., "Forecasting the Weather: The Relationship of Temperature and Circulation Aloft," *Weatherwise*, vol. 3, Nos. 4-6, August-December 1950, pp. 89-92, 113-116, 138-141.
4. C. K. Stidd, "The Use of Correlation Fields in Relating Precipitation to Circulation," *Journal of Meteorology*, vol. 11, No. 3, June 1954, pp. 202-213.

## SOME SMALL-SCALE FEATURES OF THE TRACK OF HURRICANE IONE

HAROLD M. JORDAN AND DAVID J. STOWELL

National Weather Analysis Center, U. S. Weather Bureau, Washington, D. C.

### 1. INTRODUCTION

Ione was named on the 14th of September 1955. Previously, on September 10, the existence of a tropical disturbance near  $11^{\circ}$  N.,  $45^{\circ}$  W. had been suspected. The next day reconnaissance aircraft located a center at  $15^{\circ} 35'$  N.,  $50^{\circ} 35'$  W. Thereafter the developing storm moved west-northwestward at about 10 knots until the 17th when it was north of the Bahamas. During the 17th it turned gradually and moved north-northwest at 13 knots until it entered the coast of North Carolina on the morning of the 19th. During the 19th Ione stopped, recurved, and moved out into the North Atlantic. On the 21st Ione lost her name and disappeared into an extratropical deep Low off Newfoundland.

For some 35 hours, from the 18th at 1945 EST until the 20th at 0643 EST, the eye of Ione was under surveillance of the new radar installation at Hatteras, N. C. For part of that time the center was in an area of many surface observing stations. It was here that several oscillations and finally recurvature took place. This study will examine some of the small-scale features of the vacillations in this segment of the track of Ione.

### 2. ANALYSIS OF DATA

Several radar stations reported fixes on Ione. These fixes were made by Navy and Air Force installations as well as by the Weather Bureau. Because of the greater proximity of the Hatteras radar<sup>1</sup> station to the area of interest in this paper, all the fixes from this station are presented in figure 1 exactly as they were plotted by Mr. Vaughn Rockney of the Weather Bureau who made most of the eye observations at the radar site. Figure 2 is an analysis of the track of the radar fixes of the eye of Ione. The positions in figure 1 are augmented in a few places by examination of a time lapse movie made simultaneously.

It can be seen from figures 1 and 2 that prior to 0630 EST of the 19th the movement was mainly north-northwest at 14 knots; from 0630 to 1130 EST it was nearly stationary while several oscillations took place; and from 1130 to 1830 EST it was mainly north-northeast at 10 knots. From 1930 to 2230 EST more oscillations occurred and

subsequent to 2230 EST Ione accelerated east-northeastward. During the period from 0430 to 1330 EST the eye was very close to the observing stations on the North Carolina coast at Morehead City, Cherry Point, New Bern, Kinston, Wilmington, and Hatteras. Also during this period any deepening or filling of the storm was very slight, so that any pressure changes recorded at the stations most likely reflect features of general movement of the storm.

Figure 3 is a collection of pressure profiles at some of the stations in the vicinity of the storm center. These profiles are reduced to one horizontal time scale, but the vertical scale is only relative, the reference having been shifted for each station to separate the traces. Pressure readings taken by the cooperative observer at Morehead City were at irregular intervals and since no barograph trace is available the profile cannot be presented.

An examination of the profiles shows:

1. Large pressure falls at all stations in advance of the center until 0630 EST on the 19th.
2. Only slight pressure changes at all stations from 0630 to 1130 EST on the 19th.
3. Large pressure rises at stations behind the center after 1130 EST.

Surface isobaric analyses of sequence reports, light ships, and ships at sea were made in the Analysis Center each hour during the progress of Ione through the North Carolina coastal area. These analyses were revised where necessary after receipt by mail of all additional hourly reports from the stations which were unable to transmit them by teletypewriter. Copies of the hourly analyses, with the track from figure 2 superimposed, are presented in figure 4. Plotted at each station is the 1-hour pressure change during the hour preceding map time.

The hourly isobaric analyses agree closely with the radar fixes. The hourly tendencies, wind changes, and synchronous pressure fluctuations on the original barograms agree closely with the movements indicated by the radar fixes.

The sea level isobars at 0430, 0530, and 0630 EST show the pressure center of Ione south-southeast of Cherry Point (NKT) and Morehead City and as near to the radar fixes as can be determined by the surface network. One-hour pressure falls were large and increasing ahead of the center at Cherry Point and New Bern (EWN).

<sup>1</sup> Model SPIM, wave length 10 cm., beam width  $3^{\circ}$ , peak power 750,000 watts, antenna size 8 ft., pulse length 5 microseconds.

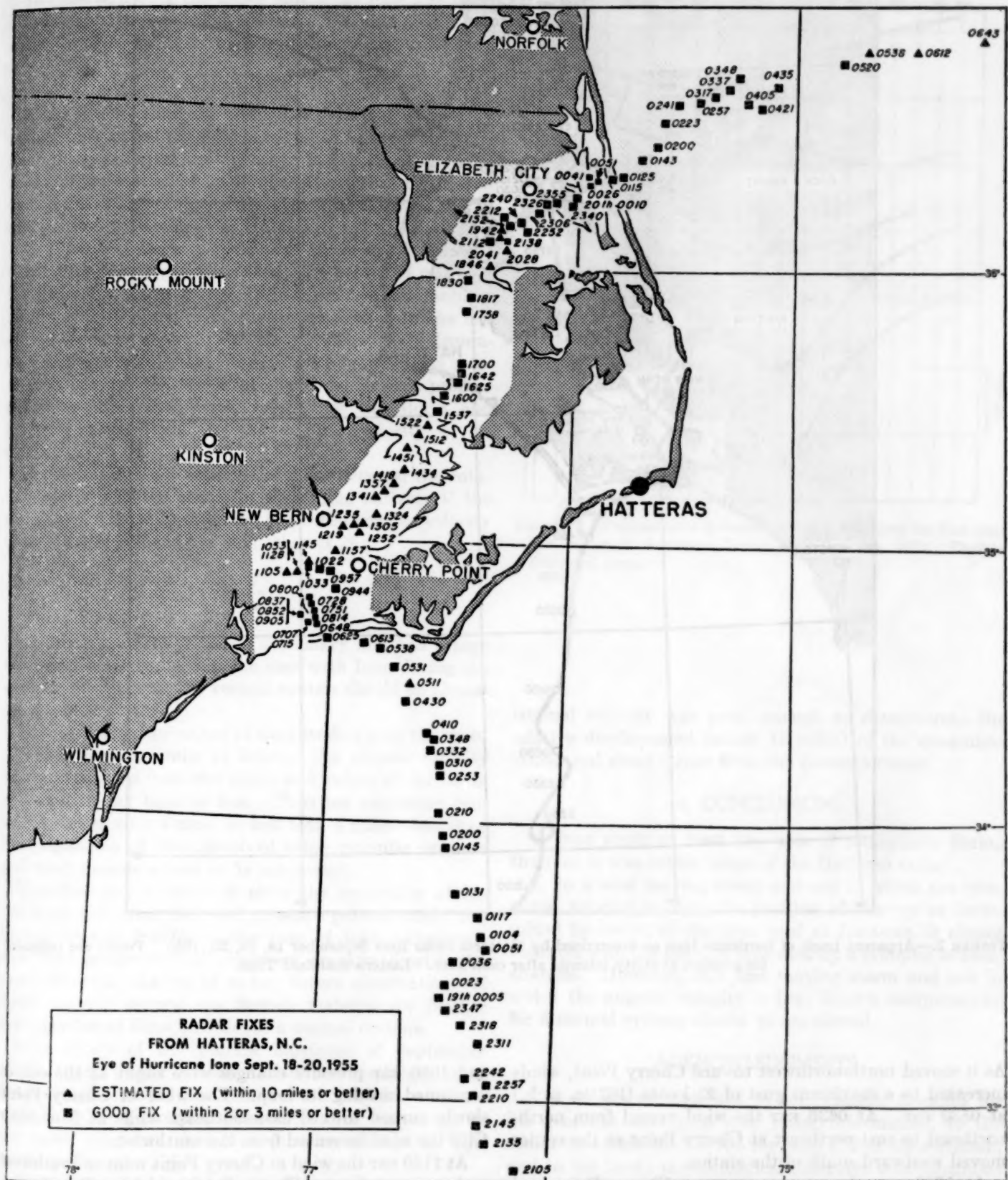


FIGURE 1.—Positions of the eye of hurricane Ione as determined by Hatteras radar, September 18, 19, 20, 1955. Eastern Standard Time.

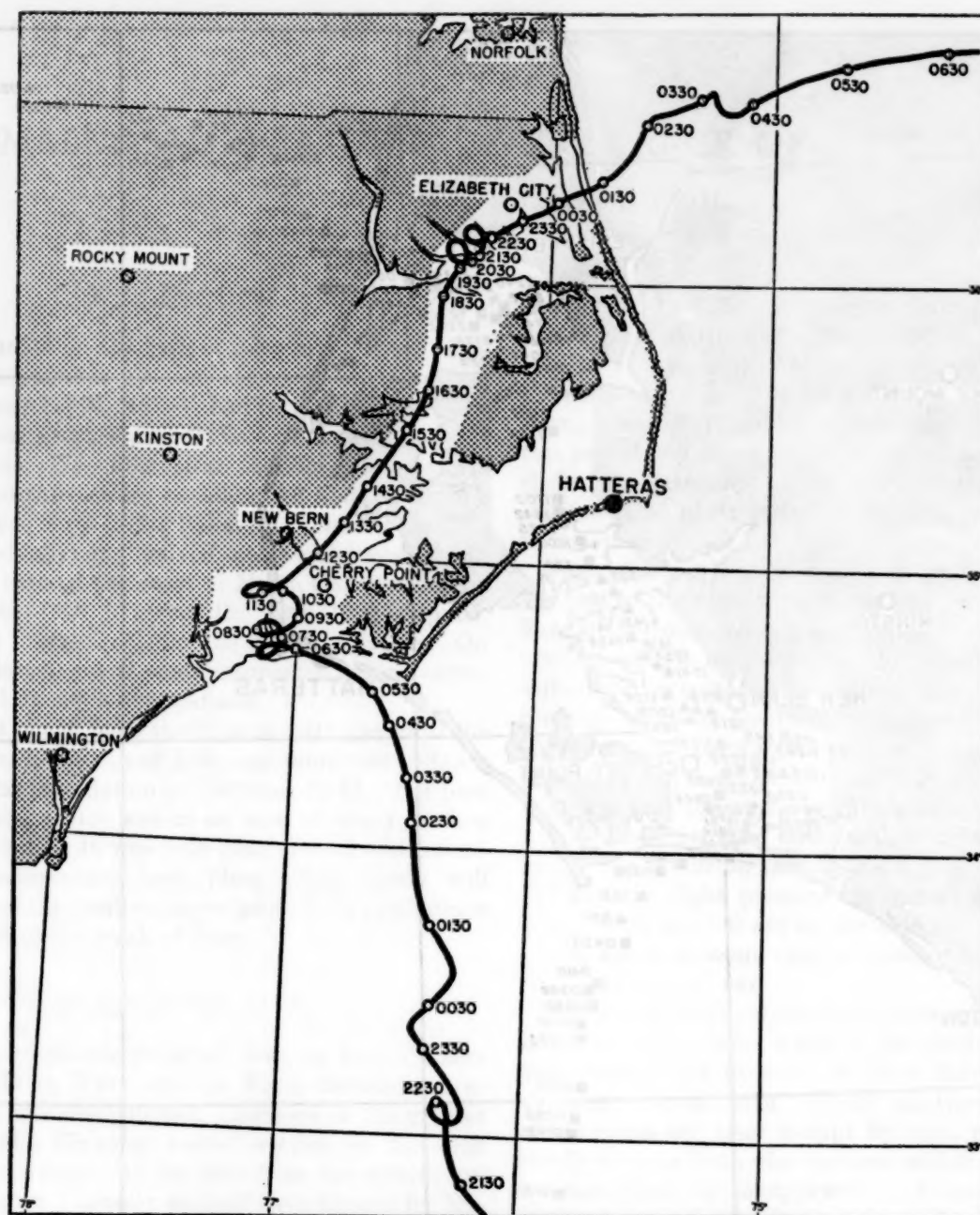


FIGURE 2.—Apparent track of hurricane Ione as determined by Hatteras radar fixes September 18, 19, 20, 1955. Points are indicated for position at thirty minutes after each hour. Eastern Standard Time.

As it moved north-northwest toward Cherry Point, winds increased to a maximum gust of 93 knots (107 m. p. h.) at 0530 EST. At 0630 EST the wind veered from north-northeast to east-northeast at Cherry Point as the center moved westward south of the station.

At 0730 EST the pressure rose at Cherry Point and fell less rapidly at New Bern as the center moved more slowly and away from Cherry Point. At 0830, 0930,

and 1030 EST pressure changes were slight as the center continued making its loop. The wind at Cherry Point slowly turned toward east-southeast while at Morehead City the wind increased from the southwest.

At 1130 EST the wind at Cherry Point went to southwest and pressure rises at Cherry Point and New Bern began to increase just prior to 1230 EST as the center accelerated north-northeastward.

In general, during the entire time while Ione was being watched by the radar at Hatteras the center did not differ from the radar fix by any discernible distance.

### 3. RADAR AND TROPICAL STORMS

There is more than one method of observing a storm by radar. A study of the echo pattern can be made to determine the position of the open eye in the cloud and rain shield, or the motion of small separate cells can be tracked to determine the center of the streamline pattern. The first method was utilized at Hatteras.

In a tropical storm the cloud and rain eye is believed to be most nearly concentric with the center of rotation. In a moving storm this is to the right of the isobaric center while the center of the streamlines is to the left of the isobaric center. Sir Napier Shaw [1,2] demonstrated geometrically that the distance between the rotation center and the center of the streamlines is proportional to the translational velocity of the storm and inversely proportional to the angular velocity of its rotation.

If  $s$  is the distance in nautical miles between the rotation center and the center of streamline pattern,  $V$  the translational velocity in knots, and  $\omega$  the angular velocity of rotation in radians per hour, then [1,2]

$$s = \frac{V}{\omega}$$

Thus when a storm is nearly stationary and has a high rotational velocity, as was the case with Ione during the morning of the 19th, the various centers should be almost coincident.

In Ione during the period of time studied here the speed of translation was under 15 knots. The angular velocity can be estimated from the winds and radius of the storm at 4 radians per hour or less. Thus the maximum estimated distance for  $s$  must be less than 4 miles—less than the magnitude of error involved using synoptic pressure and wind considerations to fix the center.

Therefore any attempt to show the separation of the eye from the wind field and pressure pattern could not be particularly fruitful in the case of Ione. However, now that meteorological observers are armed with the more accurate weapon of radar, future observations of faster moving storms can furnish material for further investigation of Shaw's model of a normal cyclone.

In a study of the Florida hurricane of September 14-15, 1945, Wexler [3] found that the displacement of the paths of pressure and radar centers may have agreed with Shaw's explanation when the storm was north of the radar site, but showed a puzzling change in sign south of the radar site.

Hatakeyama et al. [4] present an observational case of a fast moving storm. In this typhoon (Lorna) the trans-

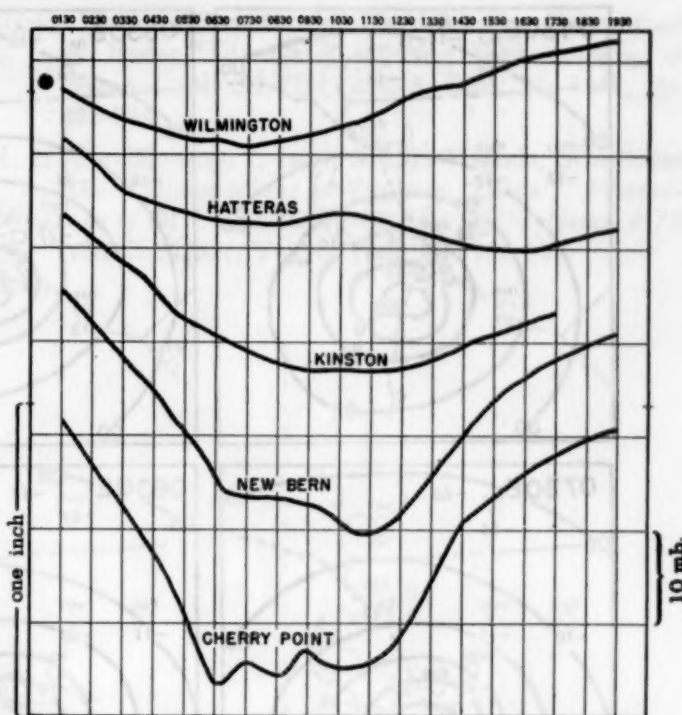


FIGURE 3.—Comparative pressure profiles for various stations near the center of hurricane Ione, September 19, 1955. Eastern Standard Time.

lational velocity was great enough to demonstrate the relative displacement (about 15 miles) of the streamline center and cloud center from the pressure center.

### 4. CONCLUSIONS

1. Ione made at least two sets of oscillations during the time it was within range of the Hatteras radar.
2. In a slow moving storm and one in which the rotational velocity is high, the position of the eye as determined by radar, of the type used at Hatteras, is almost identical with the position indicated by a synoptic isobaric analysis. However, in a fast moving storm and one in which the angular velocity is low, Shaw's computations for a normal cyclone should be considered.

### ACKNOWLEDGMENTS

The writers are indebted to Mr. Vaughn Rockney for his generous assistance with radar information, to the senior members of NWAC for advice and consultation, and to the hardy meteorological observers who continued to log regular reports as Ione passed almost directly over them.

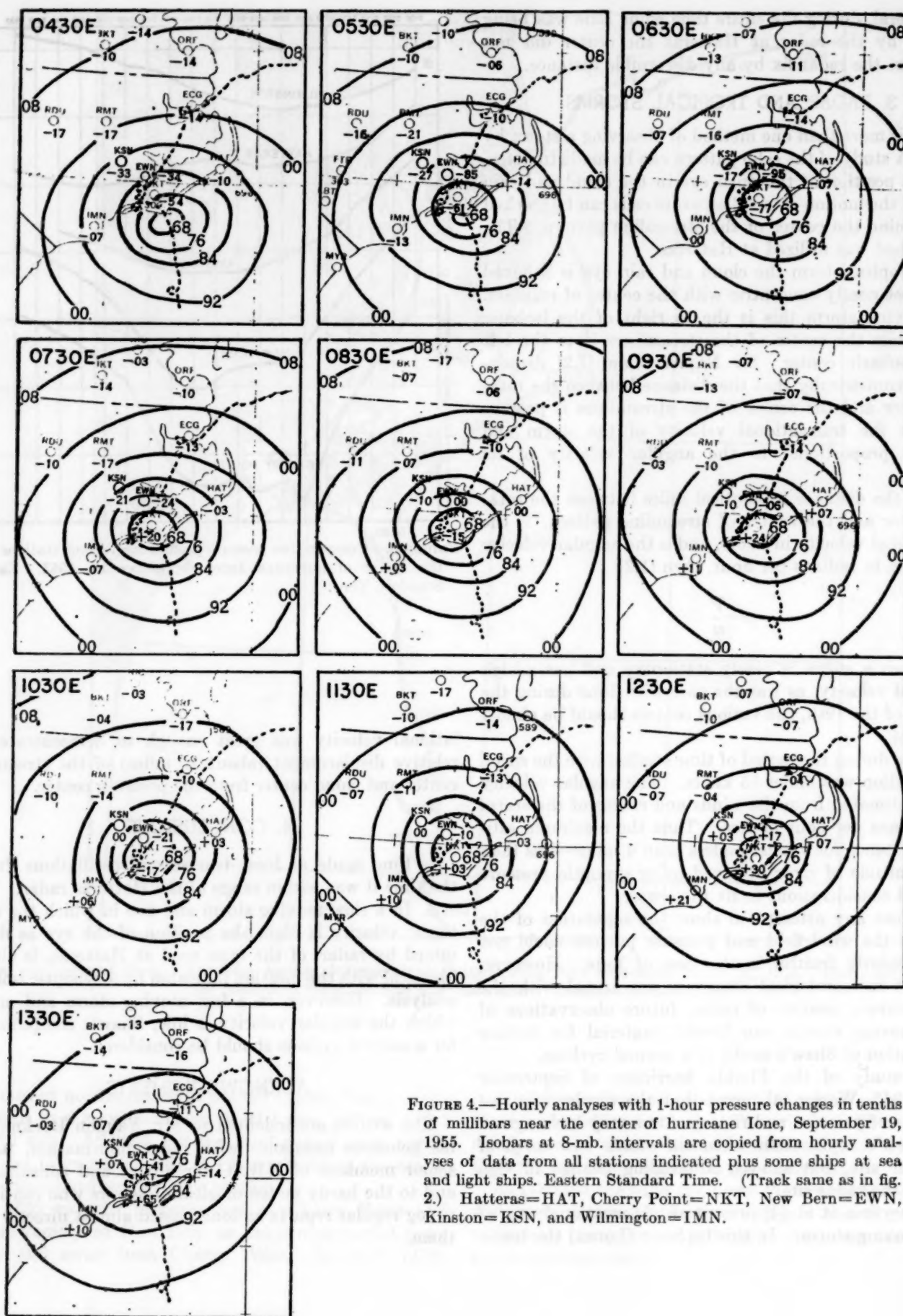


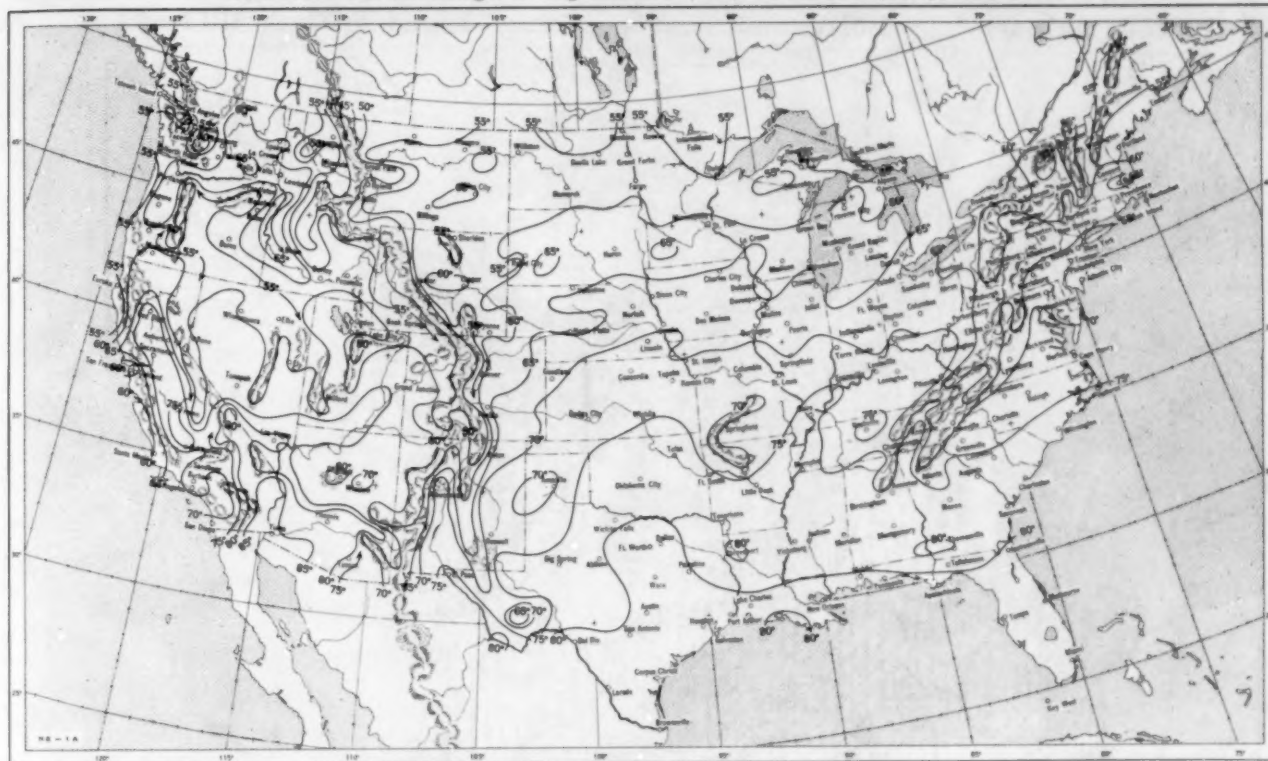
FIGURE 4.—Hourly analyses with 1-hour pressure changes in tenths of millibars near the center of hurricane Ione, September 19, 1955. Isobars at 8-mb. intervals are copied from hourly analyses of data from all stations indicated plus some ships at sea and light ships. Eastern Standard Time. (Track same as in fig. 2.) Hatteras=HAT, Cherry Point=NKT, New Bern=EWN, Kinston=KSN, and Wilmington=IMN.

## REFERENCES

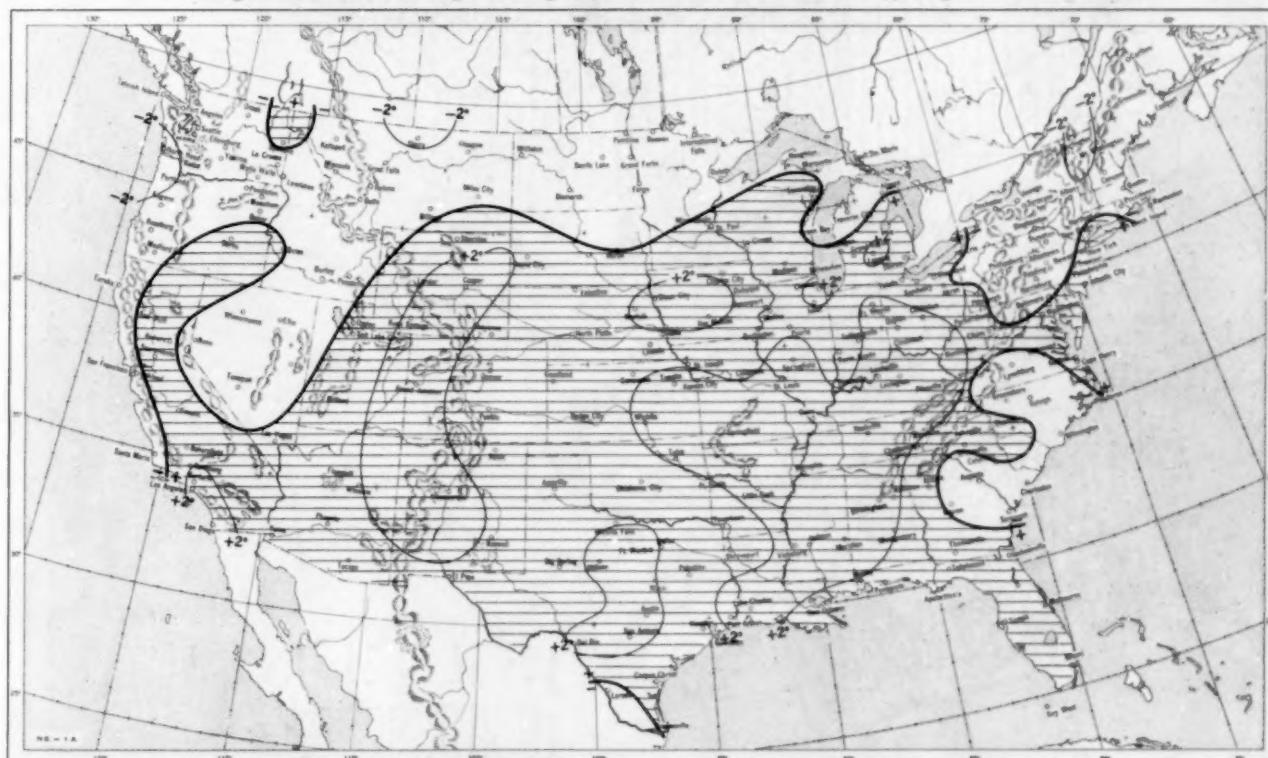
1. W. N. Shaw, "Curved Isobars," Ch. IX of *Manual of Meteorology* Part IV, University Press, Cambridge, 1931, pp. 231-249.
2. W. N. Shaw, "The Travel of Circular Depressions and Tornadoes and the Relation of Pressure to Wind for Circular Isobars," *Geophysical Memoirs* No. 12, British Meteorological Office, London, 1918, 44 pp.
3. H. Wexler, "Structure of Hurricanes as Determined by Radar," *Annals of the New York Academy of Sciences*, vol. XLVIII, Art. 8, Sept. 15, 1947, pp. 821-844.
4. H. Hatakeyama, I. Imai, and Y. Masuda, "On Some Radar Observations of Typhoon 'Lorna'," *Proceedings of the UNESCO Symposium on Typhoons, 9-12 November 1954*, Tokyo, 1955, pp. 121-128.



Chart I. A. Average Temperature ( $^{\circ}\text{F.}$ ) at Surface, September 1955.



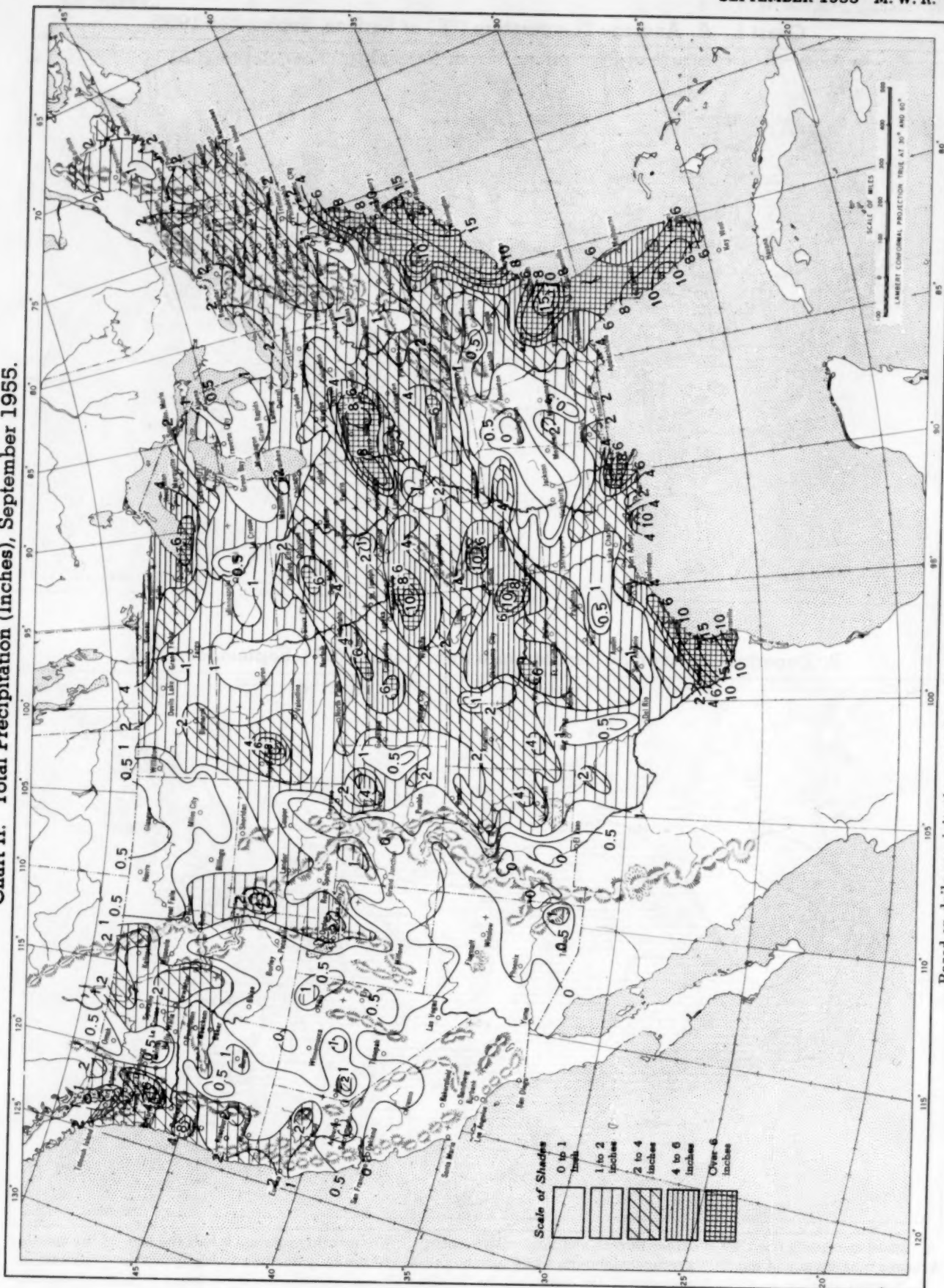
B. Departure of Average Temperature from Normal ( $^{\circ}\text{F.}$ ), September 1955.



A. Based on reports from 800 Weather Bureau and cooperative stations. The monthly average is half the sum of the monthly average maximum and monthly average minimum, which are the average of the daily maxima and daily minima, respectively.

B. Normal average monthly temperatures are computed for Weather Bureau stations having at least 10 years of record.

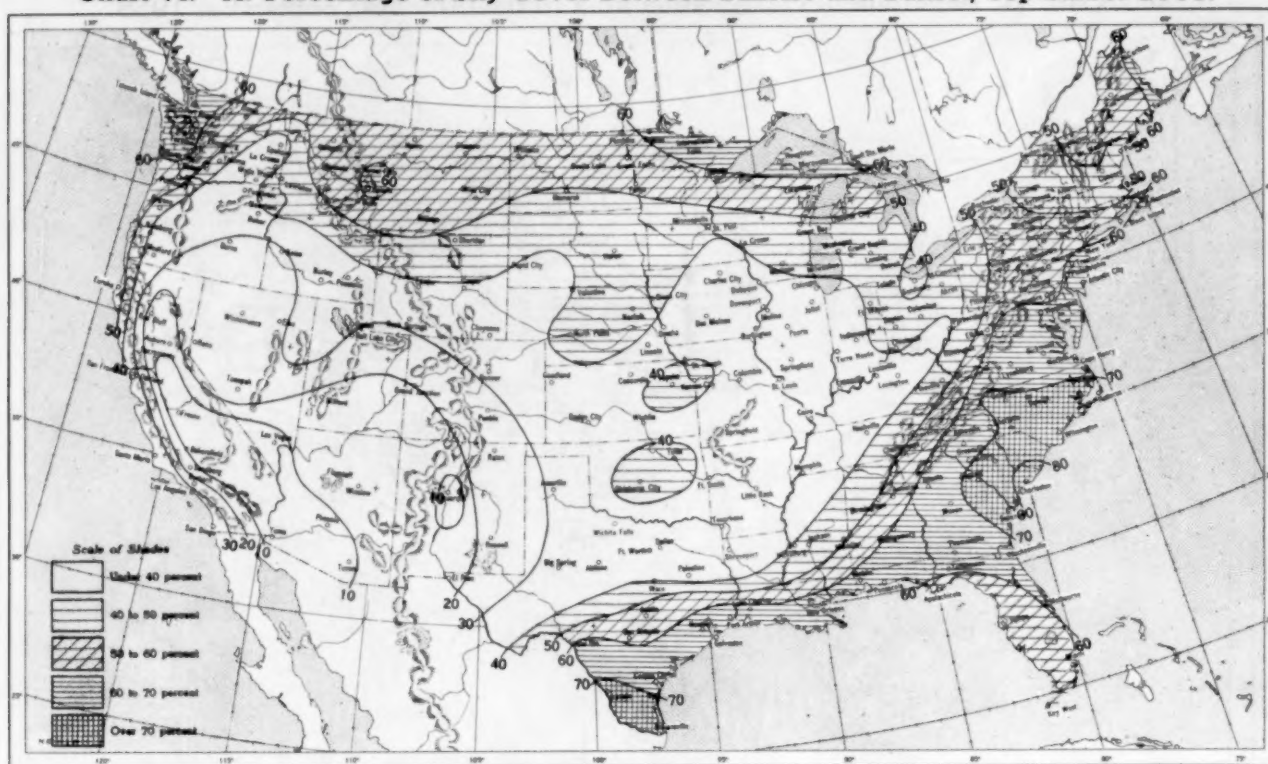
Chart II. Total Precipitation (Inches), September 1955.



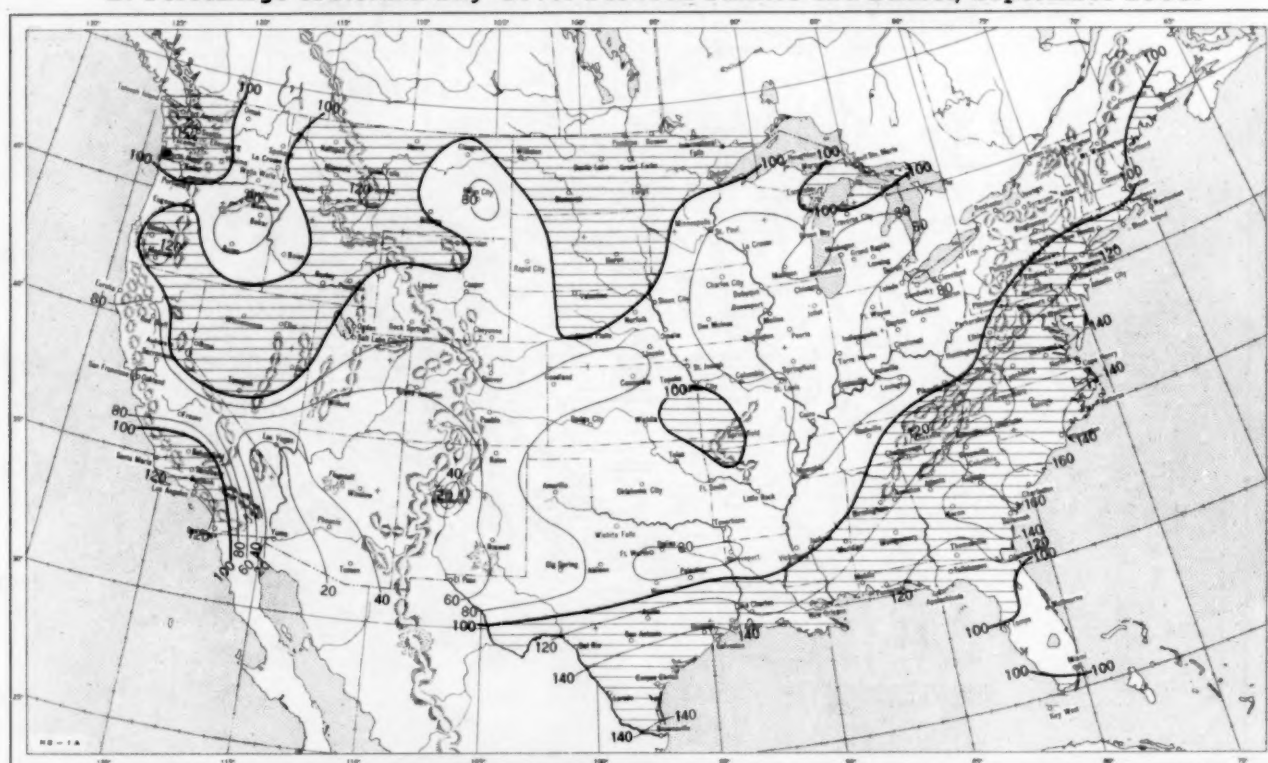
Based on daily precipitation records at 800 Weather Bureau and cooperative stations.



Chart VI. A. Percentage of Sky Cover Between Sunrise and Sunset, September 1955.

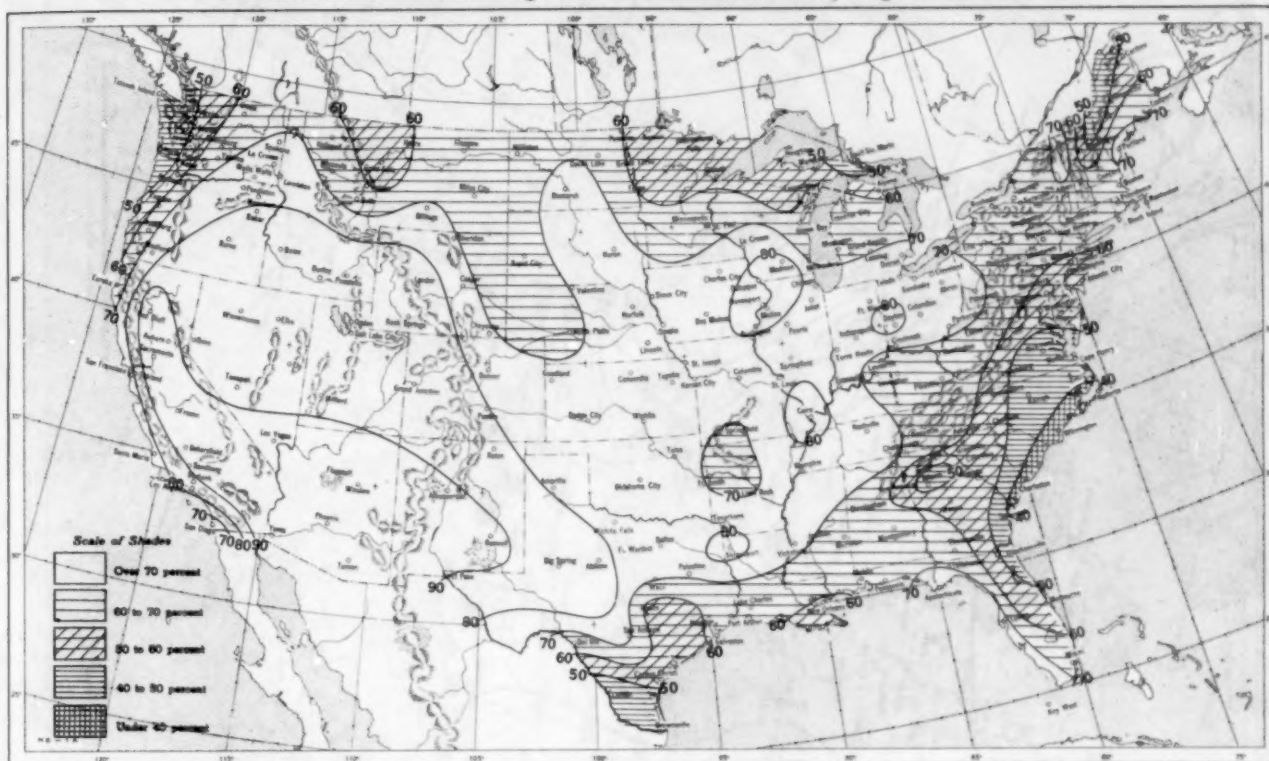


B. Percentage of Normal Sky Cover Between Sunrise and Sunset, September 1955.

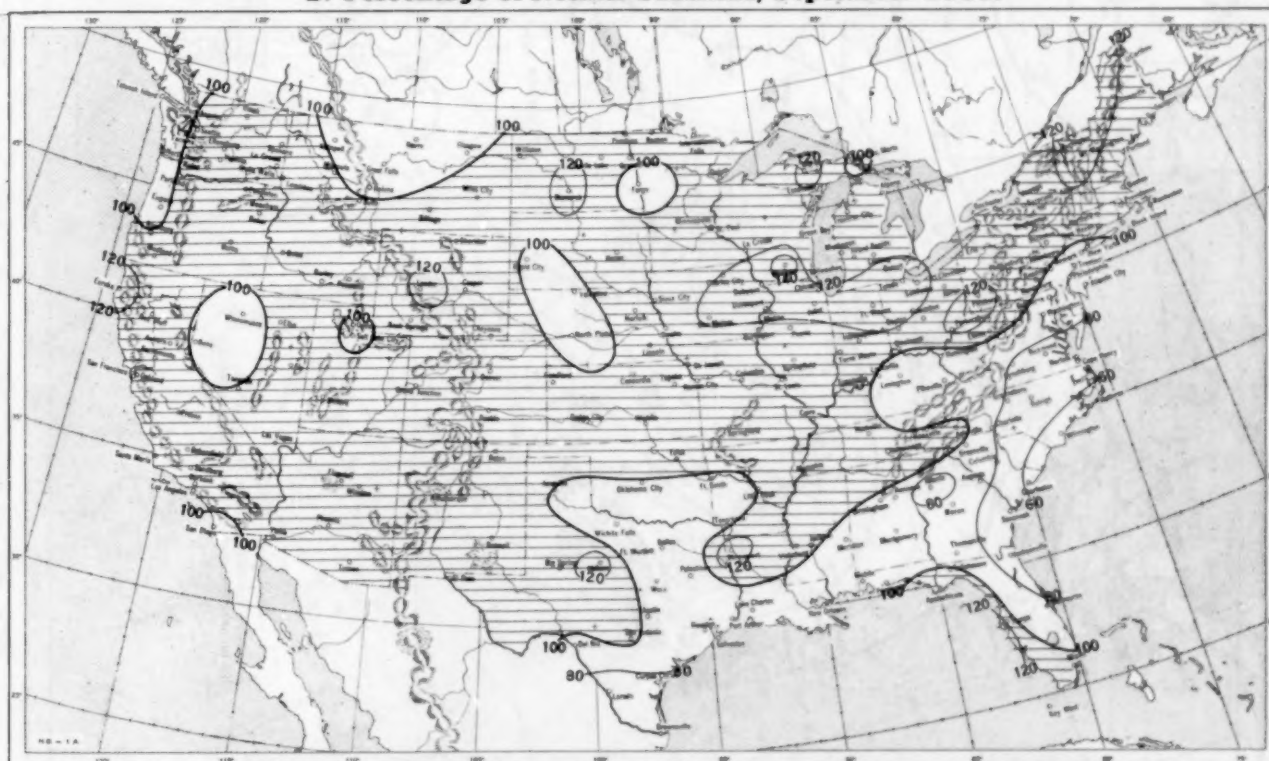


A. In addition to cloudiness, sky cover includes obscuration of the sky by fog, smoke, snow, etc. Chart based on visual observations made hourly at Weather Bureau stations and averaged over the month. B. Computations of normal amount of sky cover are made for stations having at least 10 years of record.

Chart VII. A. Percentage of Possible Sunshine, September 1955.

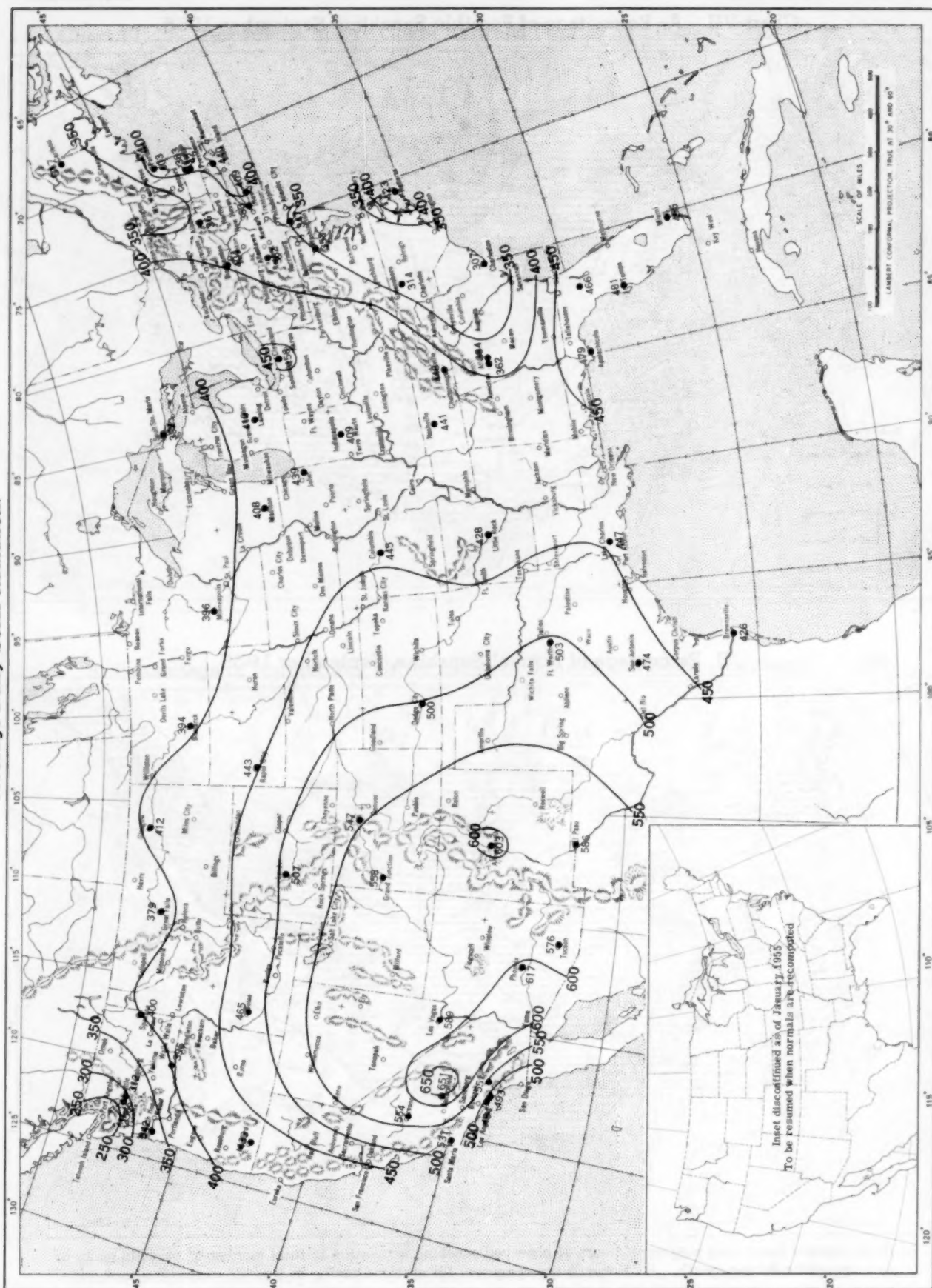


B. Percentage of Normal Sunshine, September 1955.



A. Computed from total number of hours of observed sunshine in relation to total number of possible hours of sunshine during month. B. Normals are computed for stations having at least 10 years of record.

Chart VIII. Average Daily Values of Solar Radiation, Direct + Diffuse, September 1955. Inset: Percentage of Normal Average Daily Solar Radiation.



Circle indicates position of center at 7:30 a. m. E. S. T. Figure above circle indicates date, figure below, pressure to nearest millibar. Dots indicate intervening 6-hourly positions. Squares indicate position of stationary center for period shown. Dashed line in track indicates reformation at new position. Only those centers which could be identified for 24 hours or more are included.

Chart IX. Tracks of Centers of Anticyclones at Sea Level, September 1955.

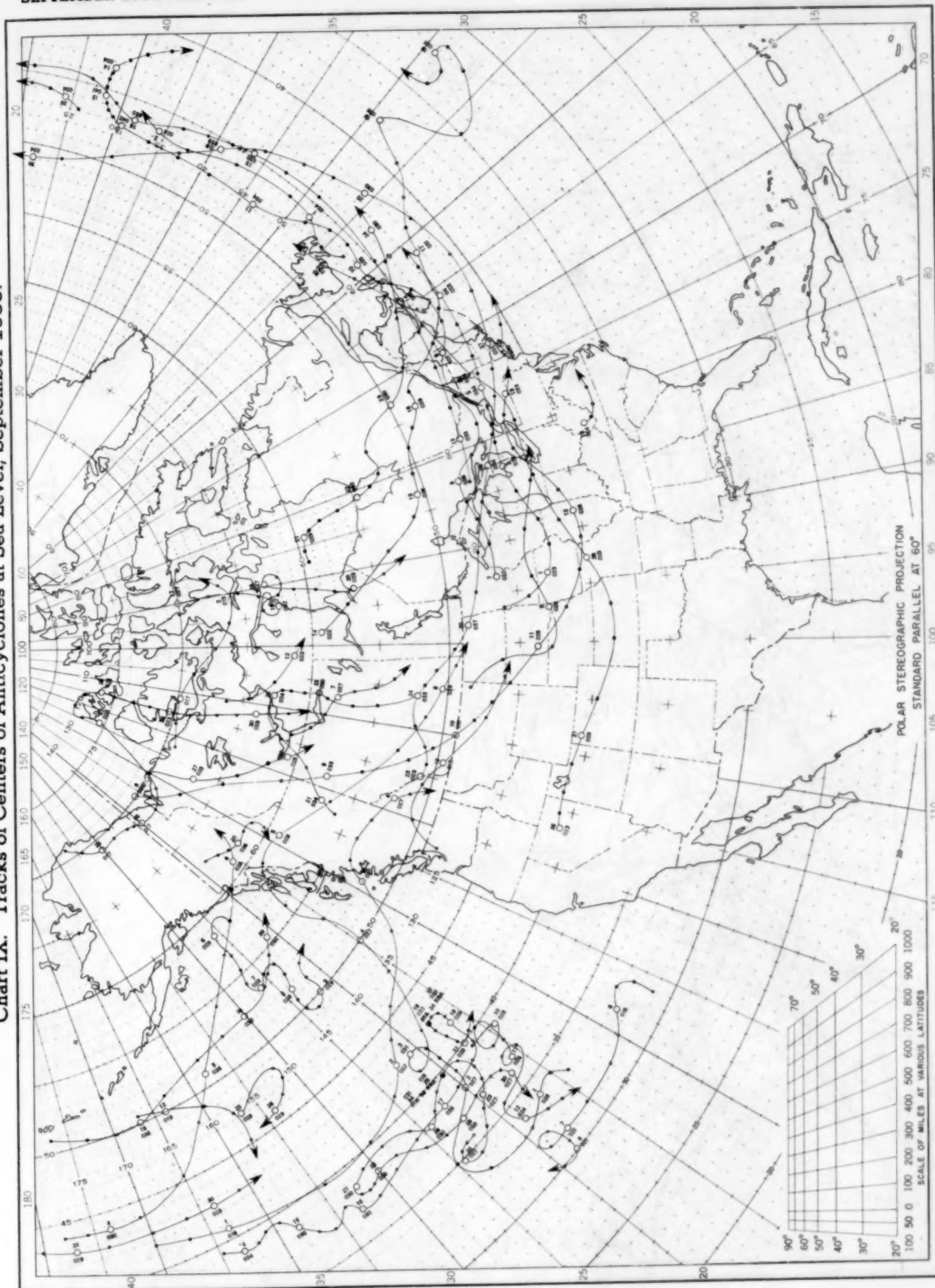


Chart shows mean daily solar radiation, direct + diffuse, received on a horizontal surface in langley (1 langley = 1 gm. cal. cm. <sup>-2</sup>). Basic data for isolines are shown on chart. Further estimates are obtained from supplementary data for which limits of accuracy are wider than for those data shown.

Chart X. Tracks of Centers of Cyclones at Sea Level, September 1955.

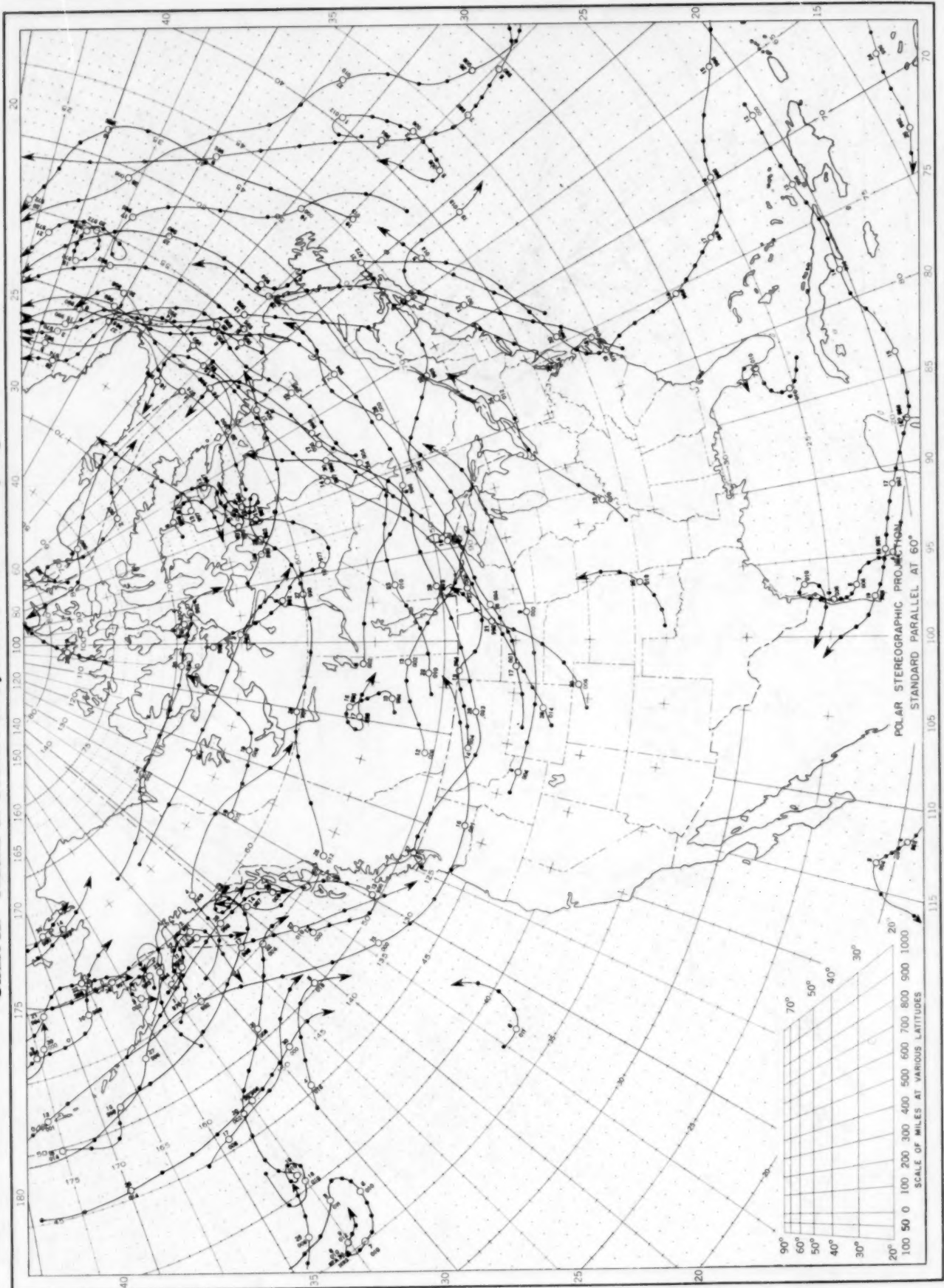
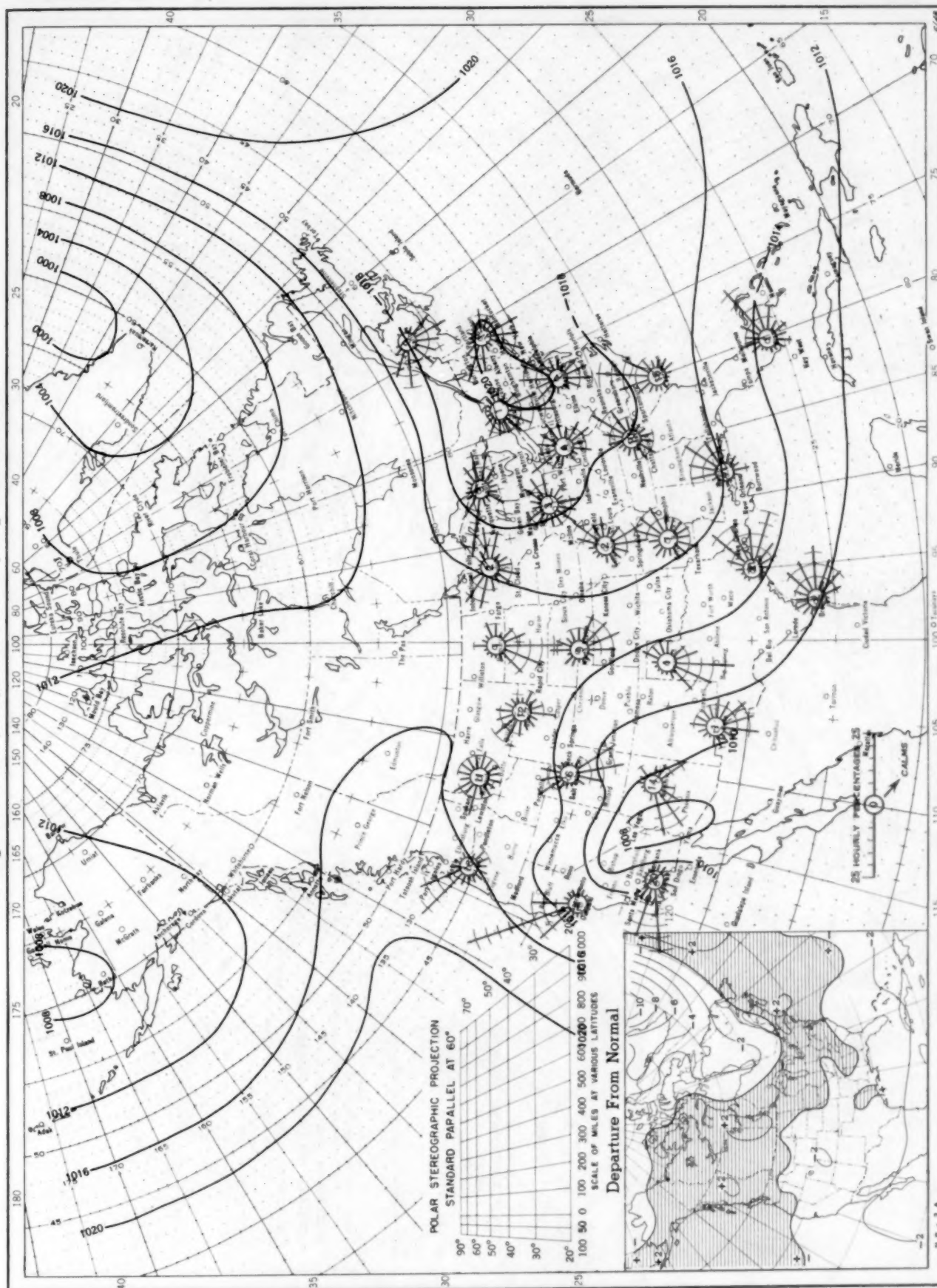
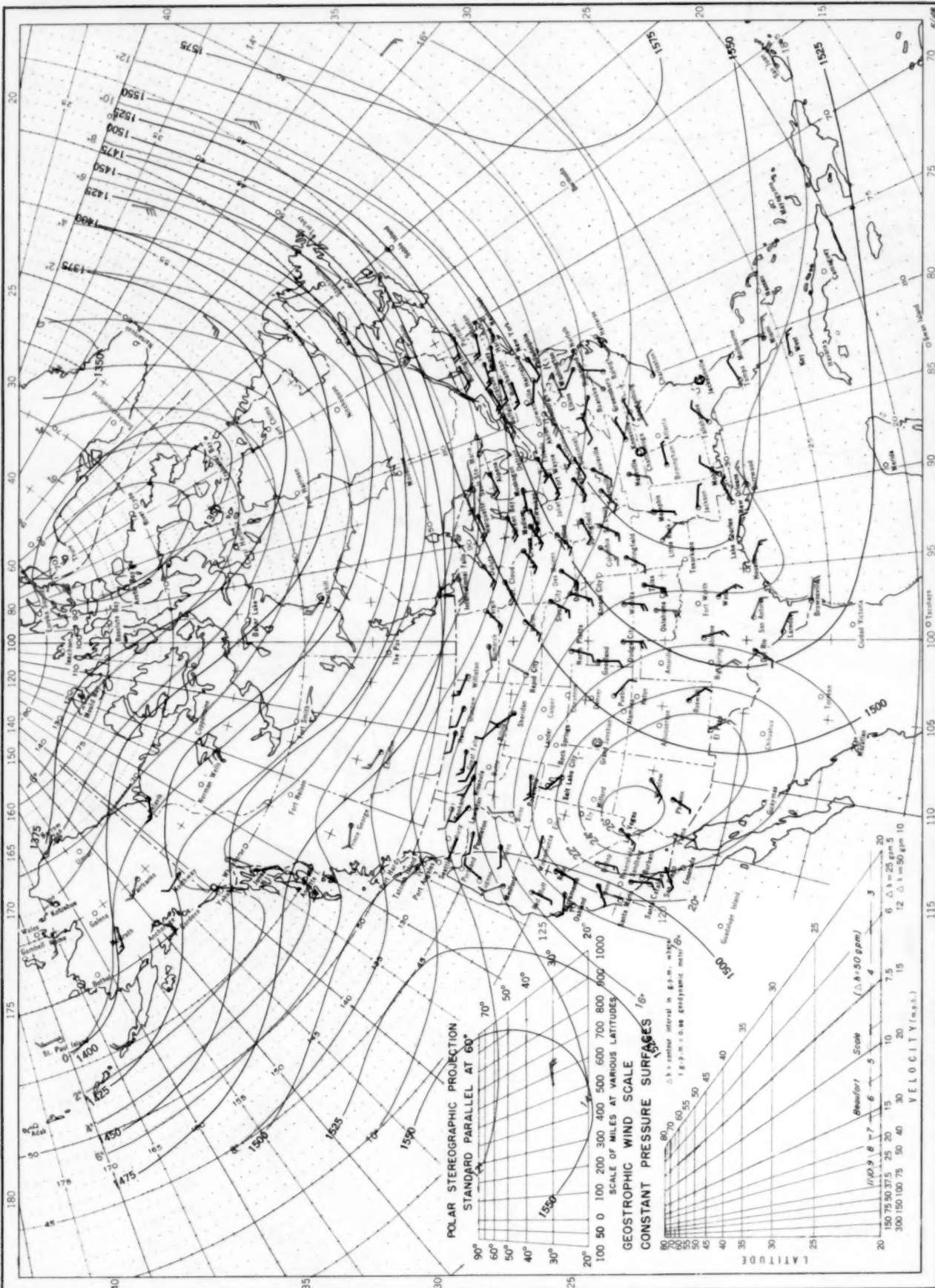


Chart XI. Average Sea Level Pressure (mb.) and Surface Windroses, September 1955. Inset: Departure of Average Pressure (mb.) from Normal, September 1955.



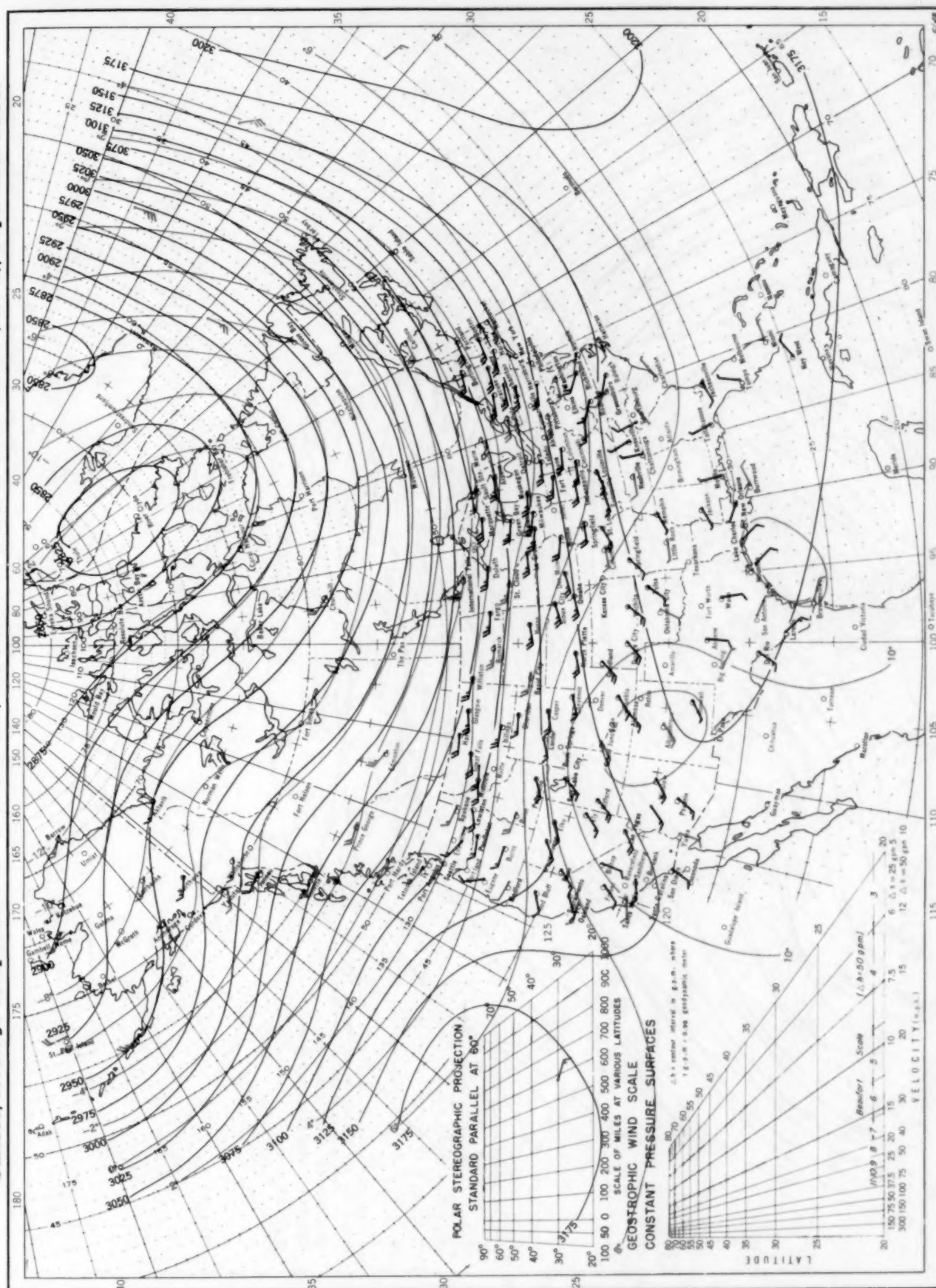
Average sea level pressures are obtained from the averages of the 7:30 a. m. and 7:30 p. m. E. S. T. readings. Windroses show percentage of time wind blew from 16 compass points or was calm during the month. Pressure normals are computed for stations having at least 10 years of record and for 10° inter-sections in a diamond grid based on readings from the Historical Weather Maps (1899-1939) for the 20 years of most complete data coverage prior to 1940.

Chart XII. Average Dynamic Height in Geopotential Meters (1 g.p.m. = 0.98 dynamic meters) of the 850-mb. Pressure Surface, Average Temperature in °C. at 850 mb., and Resultant Winds at 1500 Meters (m.s.l.) September 1955.



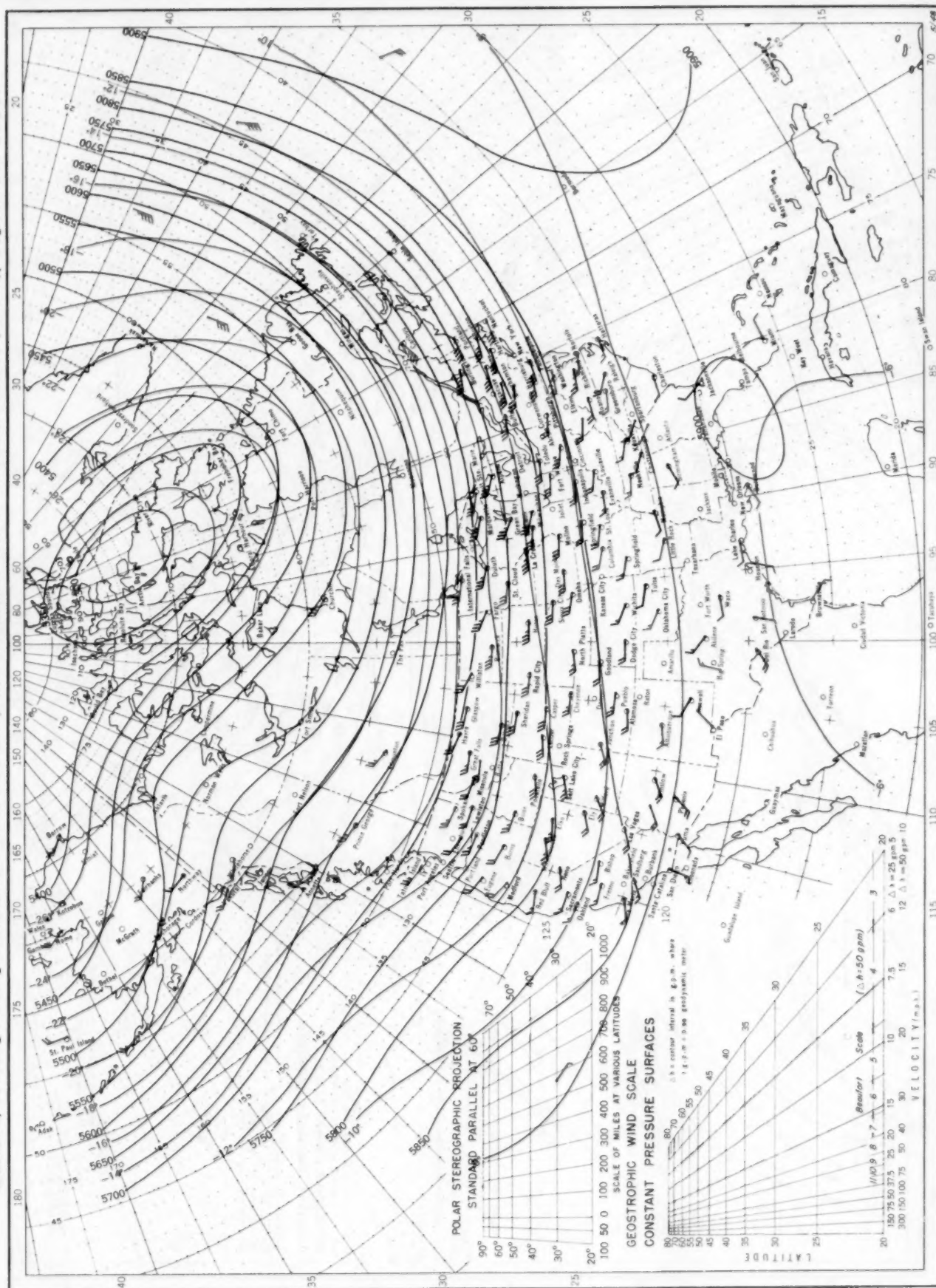
Contour lines and isotherms based on radiosonde observations at 0300 G. M. T. Winds shown in black are based on pilot balloon observations at 2100 G. M. T.; those shown in red are based on rawins taken at 0300 G. M. T. Wind barbs indicate wind speed on the Beaufort scale.

Chart XIII. Average Dynamic Height in Geopotential Meters (1 g.p.m. = 0.98 dynamic meters) of the 700-mb. Pressure Surface, Average Temperature in °C. at 700 mb., and Resultant Winds at 3000 Meters (m.s.l.), September 1955.



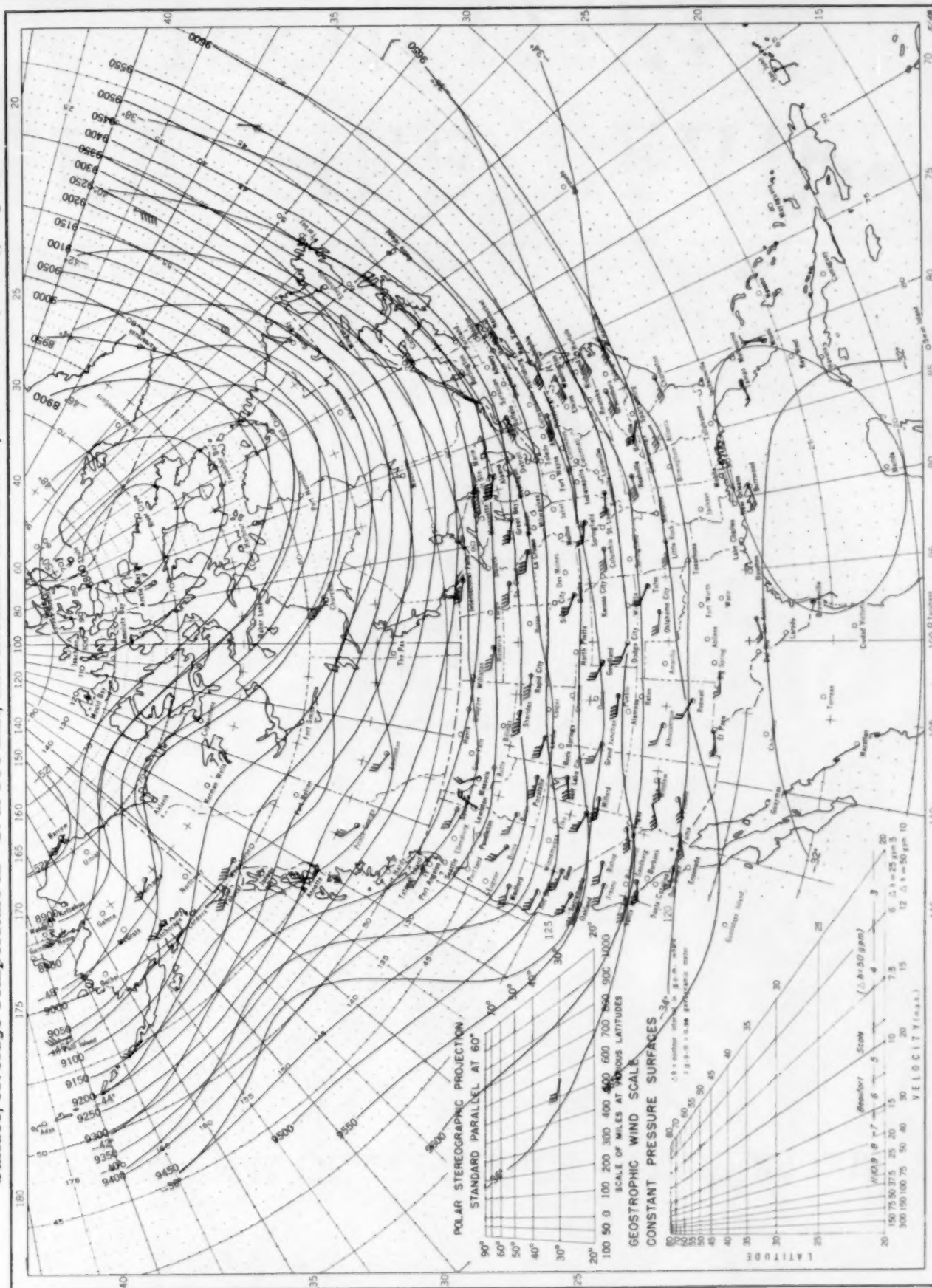
Contour lines and isotherms based on radiosonde observations at 0300 G. M. T. Winds shown in black are based on pilot balloon observations at 2100 G. M. T.; those shown in red are based on rawins taken at 0300 G. M. T. Wind barbs indicate wind speed on the Beaufort scale.

Chart XIV. Average Dynamic Height in Geopotential Meters (1 g.p.m. = 0.98 dynamic meters) of the 500-mb. Pressure Surface, Average Temperature in °C. at 500 mb., and Resultant Winds at 5000 Meters (m.s.l.), September 1955.



Contour lines and isotherms based on radiosonde observations at 0300 G. M. T. Winds shown in black are based on pilot balloon observations at 2100 G. M. T.; those shown in red are based on rawinsonde observations at 0300 G. M. T. Wind barbs indicate wind speed on the Beaufort scale.

Chart XV. Average Dynamic Height in Geopotential Meters (1 g.p.m. = 0.98 dynamic meters) of the 300-mb. Pressure Surface, Average Temperature in °C. at 300 mb., and Resultant Winds at 10,000 Meters (m.s.l.), September 1955.



Contour lines and isotherms based on radiosonde observations at 0300 G. M. T. Winds shown in black are based on pilot balloon observations at 2100 G. M. T.; those shown in red are based on rawins at 0300 G. M. T. Wind barbs indicate wind speed on the Beaufort scale.